Eberhard Karls Universität Tübingen

Mathematisch-Naturwissenschaftliche Fakultät

Institut für Theoretische Physik

BACHELOR THESIS

Time-crystal phase transition and quantum correlations in a driven-dissipative spin-boson model

by Robert Mattes

Supervisors: Dr. Federico Carollo
Prof. Dr. Igor Lesanovsky

30th January 2023

Declaration of Authenticity

I hereby declare that I have written this bachelor thesis independently and without the use of sources other than those indicated. All quotes that have been taken verbatim or in content from other works I have marked as such. This thesis has not yet been submitted in the same or a similar form to any other university as an examination. So far, this work has not been published.

Tübingen, 30th January 2023	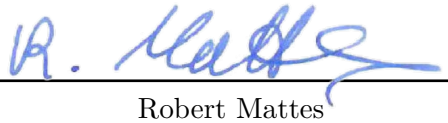
Place, Date	Robert Mattes

Contents

1. Introduction

For more than half a century theoretical physicists investigated systems consisting of atoms coupled to a light field [1–4]. These models revealed intriguing equilibrium as well as ground state phase transitions towards so-called superradiant phases, i.e. phases where the light field features a macroscopic number of excitations. Recently, also due to challenges in the possibility of experimentally realizing interesting light-atom interactions, open quantum versions of these models are receiving much attention [5, 6]. In this setting, dissipative processes due to the coupling between the system and the bath have to be taken into account.

In the Markovian case, dissipation usually leads to irreversibility and convergence of the quantum state of the system towards a stationary state. However, recent results pointed to the possibility of the emergence of non-stationary behavior [7] and of nonequilibrium phase transitions towards quantum many-body phases in which the system does not reach a stationary state for long times, but rather undergoes persistent oscillations [8, 9]. The convergence of the system state to a limit cycle implies that these many-body phases break the continuous time-translation symmetry of the generator of the Markovian dynamics. Therefore, these systems give rise to a crystalline structure in time and are thus often referred to as time-crystals [7, 8].

The first proposal of a time-crystal [10] involved equilibrium systems. However, it was later shown via a no-go theorem that these new phases of quantum matter are actually impossible in equilibrium [11, 12]. Despite this fact, the idea of a self-ordered system in time, similar to ordering in space in condensed matter, was the starting point for many studies. It was shown that time-crystals can occur in periodically driven closed systems where the discrete time-translation symmetry of the Markov generator of the dynamics is broken. These systems are referred to discrete or Floquet time-crystals [13–15]. In open dissipative systems the formation of a crystalline structure in time can either take place as a consequence of a continuous [7, 8, 16] or discrete [17, 18] time-translation symmetry breaking. Several experiments witnessed the existence of discrete and continuous time-crystals [19–21].

A model consisting of an ensemble of spins with collective dissipation that shows a time-crystal phase is the so-called boundary time-crystal [8]. This model is the simplest one displaying a breaking of the continuous time-translation symmetry and has been therefore the subject of different studies [8, 9, 22–24]. A mean-field approach captures the dynamics of this model through a set of nonlinear differential equations. The corresponding mean-field operators act as order parameters to detect the phase transition from the stationary to the time-crystal phase. Going beyond a mean-field treatment, an exact study of quantum fluctuations [25, 26] is also possible. In general, quantum fluctuations provide the possibility to detect correlations in many-body systems [9], as for instance dissipatively generated collective entanglement [27, 28]. In recent studies [29] quantum correlations in the boundary time-crystal were only found in the stationary regime. It thus remains an open question whether quantum correlations can be observed in time-crystalline phases.

In the following thesis, we consider a spin-boson model which describes light interacting with matter through an excitation-exchange mechanism. It is shown that in certain parameter regimes the model features a nonequilibrium phase transition towards a time-crystal phase. Interestingly, the phase transition can be both of first-order and of second-order. Quantum fluctuations are exploited to further investigate the collective correlations between the atoms and the light field. With this approach, we found entanglement in the entire time-crystal phase.

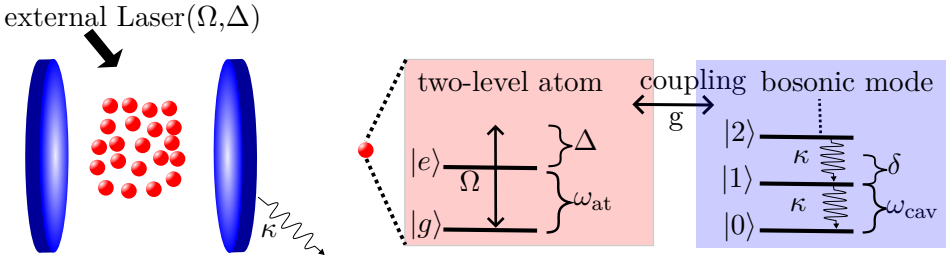

FIG. 1. **Driven-dissipative spin-boson model.** System of N two-level atoms with ground state $|g\rangle$ and excited state $|e\rangle$ coupled to an optical cavity with frequency ω_{cav} and driven by an external laser with detuning Δ and Rabi frequency Ω. The cavity is characterized by photon losses with rate κ to the environment.

Furthermore, a framework is provided to bring the fluctuations into a canonical bosonic form since for fluctuations in this form an analysis of correlations is possible. The canonical bosonic form for the fluctuations is achieved by going into a rotated frame. With the emergent model the unbounded evolution of fluctuations with time is shown. Additionally, we derived a generator for the dynamics of quantum fluctuations. This generator is asymptotically non-Markovian in the time-crystal phase due to a persistent time-dependence of the order parameters. Whereas, the time-dependence of the dynamical generator vanishes in the stationary phase such that the dynamics of the fluctuations become asymptotically Markovian.

The thesis starts with the introduction of the considered model and its dynamics defined through the Markovian quantum master equation in Sec. 2. Subsequently, the mean-field operators are introduced and the corresponding equations of motion (i.e. mean-field equations) are calculated. In Sec. 3 these equations are used to identify the phase transition. After the derivation of the phase diagram the focus is in Sec. 4 on the analysis of correlations in the system. A discussion of the results is provided in Sec. 5. The Appendix consists of detailed calculations and explanations of different aspects discussed in the thesis. In Appendix A a proof of the exactness of the mean-field equations in the thermodynamic limit is given. A stability analysis via the linearized Jacobian matrix of the stationary solutions is performed in Appendix B. Detailed calculations for Sec. 4 are presented in Appendix C.

2. Model

We investigate in this thesis a model that consists of N two-level atoms with ground state $|g\rangle$, excited state $|e\rangle$ and an energy spacing of ω_{at}. These atoms are located inside a cavity characterized by a single resonant mode at frequency ω_{cav}, depicted in Fig. 1. The electromagnetic field is described by bosonic creation and annihilation operators $d^\dagger$ and d, respectively, with the usual bosonic commutation relation $\left[d, d^\dagger\right] = 1$. The two-level atoms are modeled as spin-1/2 particles with the ground state $|g\rangle$ and the excited state $|e\rangle$. Therefore the system can be effectively described by a spin-boson model. The Hamiltonian describing the interaction between the atoms and the cavity mode is

$$H_{\text{int}} = \frac{\sqrt{2}g}{\sqrt{N}}\left(dV_+ + d^\dagger V_-\right), \tag{1}$$

which represents the coupling of the two subsystems through the exchange of excitations [22, 30]. The rescaled collective spin lowering operator V_- and the corresponding raising operator V_+ are

defined as follows

$$V_\pm = \sum_{k=1}^{N} v_\pm^{[k]}, \quad \text{with} \quad v_-^{[k]} = \frac{|g\rangle\langle e|^{[k]}}{\sqrt{2}} \quad \text{and} \quad v_+^{[k]} = \frac{|e\rangle\langle g|^{[k]}}{\sqrt{2}}.$$

The prefactor $1/\sqrt{N}$ in the interaction Hamiltonian is needed to achieve a well-defined thermodynamic limit ($N \to \infty$) [9]. The atoms are further driven by an external laser with frequency ω_{las}. The latter establishes Rabi oscillations at frequency Ω between ground and excited states. In the frame rotating with the frequency of the laser, the effect on the atoms is described by the Hamiltonian [30]

$$H_{\text{las}} = \sqrt{2}\Omega\,(V_+ + V_-) - \frac{\Delta}{\sqrt{2}} V_z\,,$$

with the detuning $\Delta = \omega_{\text{las}} - \omega_{\text{at}}$ and the collective spin operator

$$V_z = \sum_{k=1}^{N} v_z^{[k]}\,, \qquad \text{with} \qquad v_z^{[k]} = \frac{|e\rangle\langle e|^{[k]} - |g\rangle\langle g|^{[k]}}{\sqrt{2}}\,.$$

Additionally, the Hamiltonian of the cavity mode in the rotating frame reads

$$H_{\text{cav}} = -\delta d^\dagger d\,,$$

with the detuning $\delta = \omega_{\text{las}} - \omega_{\text{cav}}$. Further, the cavity-atom system is characterized by a dissipative contribution accounting for photon losses with rate κ from the cavity to the environment [31].

The dynamics of the model introduced above is governed by the Markovian quantum master equation $\dot{\rho}(t) = \mathcal{L}\,[\rho(t)]$, with the state of the system represented by its density matrix $\rho(t)$ and a time-independent generator $\mathcal{L}$ [31, 32]. Therefore, the system evolves through the propagator $\Lambda(t, t_0) = \exp\left(\mathcal{L}(t - t_0)\right)$ from the initial state $\rho(t_0)$ to the final state $\rho(t) = \Lambda(t, t_0)\,[\rho(t_0)]$. Since the focus is on the dynamics of the system in the thermodynamic limit it is convenient to study the evolution of observables in the Heisenberg picture where states are time-independent and operators evolve with time. The time-evolution of operators is given by the Heisenberg equation $\frac{\mathrm{d}}{\mathrm{d}t} O(t) = \mathcal{L}^*[O(t)]$, with the adjoint generator $\mathcal{L}^*$. For the considered model, the Heisenberg equation for a general operator O takes the following form

$$\frac{\mathrm{d}}{\mathrm{d}t} O = \mathcal{L}^*\,[O] = i\,[H, O] + \kappa \left(d^\dagger O d - \frac{1}{2} \left\{ d^\dagger d, O \right\} \right), \tag{2}$$

with the Hamiltonian

$$H = \sqrt{2}\Omega\,(V_+ + V_-) - \frac{\Delta}{\sqrt{2}} V_z + \frac{\sqrt{2}g}{\sqrt{N}} \left(d V_+ + d^\dagger V_- \right) - \delta d^\dagger d\,.$$

The collective spin operators

$$V_a = \sum_{k=1}^{N} v_a^{[k]}\,, \qquad \text{with} \qquad v_a^{[k]} = \frac{\sigma_a^{[k]}}{\sqrt{2}}\,, \quad a = x, y, z\,,$$

are used to rewrite the Hamiltonian, where $V_x = V_+ + V_-$ and $V_y = (V_+ - V_-)/i$. In this way, the commutator

$$\left[v_a^{[k]}, v_b^{[h]} \right] = \delta_{kh} \sqrt{2} i \sum_c \varepsilon_{abc} v_c^{[k]}\,, \tag{3}$$

can be exploited to simplify calculations. Therefore, the Hamiltonian reads

$$H = \sqrt{2}\Omega V_x - \frac{\Delta}{\sqrt{2}} V_z + \frac{g}{\sqrt{2N}} \left((d + d^\dagger) V_x + i(d - d^\dagger) V_y \right) - \delta d^\dagger d \,. \tag{4}$$

In a recent paper [22], it has been shown that a model similar to the one introduced above undergoes a phase transition to the time-crystal phase which is characterized by the system approaching a limit cycle for long times. For this reason, in the next section we investigate the possibility of observing this phase in the present model.

3. Time-crystal phase transition

3.1. Mean-field equations

In order to observe the emergence of a time-crystal phase in the considered model suitable order parameters must be identified. A natural choice is provided by the so-called mean-field operators which account for the collective properties of the system and are also experimentally accessible [33, 34]. In the system depicted in Fig. 1, the relevant single-particle observables are the rescaled Pauli matrices v_a for the N two-level atoms and the bosonic lowering operator d for the cavity. Consequently, the mean-field variables

$$m_a^N = \frac{V_a}{N} \quad \text{with} \quad a = x, y, z \qquad \text{and} \qquad \alpha^N = \frac{d}{\sqrt{N}} \,, \tag{5}$$

are introduced to analyze the behavior of the system in the thermodynamic limit. The commutation relation $\left[\alpha^N, (\alpha^N)^\dagger\right] = 1/N$ reveals the classical character of the bosonic operators in the thermodynamic limit. Moreover, the mean-field operators m_a^N, which represent the magnetizations of the system, become classical variables in the thermodynamic limit as well. The commutator of these magnetization operators takes the form of a mean-field operator rescaled with $1/N$ and therefore vanishes in norm in the limit [33]

$$\lim_{N\to\infty} \left[m_a^N, m_b^N \right] = \lim_{N\to\infty} \sqrt{2} i \frac{m_c^N}{N} = 0 \,.$$

However, for later convenience the bosonic creation and annihilation operators are replaced by the quadrature operators of the cavity light mode $p = (d + d^\dagger)/\sqrt{2}$ and $q = i(d - d^\dagger)/\sqrt{2}$. The commutation relation for the quadrature operators q and p is with $\left[d, d^\dagger\right] = 1$, given by $[q, p] = i$. Introducing the corresponding mean-field operators

$$m_p^N = \frac{\alpha^N + (\alpha^N)^\dagger}{\sqrt{2}} \qquad \text{and} \qquad m_q^N = i \frac{\alpha^N - (\alpha^N)^\dagger}{\sqrt{2}} \,, \tag{6}$$

results in the Hamiltonian

$$H = \sqrt{2}\Omega V_x - \frac{\Delta}{\sqrt{2}} V_z + g \left(m_p^N V_x + m_q^N V_y \right) - \delta d^\dagger d \,.$$

The dynamics of the mean-field operators can be obtained by studying the time-evolution of the corresponding operators V_a, q and p. With Eq. (2) in mind, this requires the calculation of the action of the generator on the mean-field operators

$$\begin{aligned}
\mathcal{L}^* \left[m_a^N \right] &= \sum_b \left(-2\Omega \varepsilon_{xab} + \Delta \varepsilon_{zab} - \sqrt{2} g \left(m_p^N \varepsilon_{xab} + m_q^N \varepsilon_{yab} \right) \right) m_b^N \,, \\
\mathcal{L}^* \left[m_q^N \right] &= g m_x^N - \delta m_p^N - \frac{\kappa}{2} m_q^N \,, \\
\mathcal{L}^* \left[m_p^N \right] &= -g m_y^N + \delta m_q^N - \frac{\kappa}{2} m_p^N \,.
\end{aligned} \tag{7}$$

A standard approach for making progress with these equations is to exploit a mean-field ansatz. The underlying assumption is that there are no emergent correlations between these operators due to the dynamics, which gives rise to the equations

$$\begin{aligned}\dot{m}_a(t) &= \sum_b \left(-2\Omega\varepsilon_{xab} + \Delta\varepsilon_{zab} - \sqrt{2}g\left(m_p(t)\varepsilon_{xab} + m_q(t)\varepsilon_{yab}\right)\right) m_b(t)\,,\\ \dot{m}_q(t) &= g m_x(t) - \delta m_p(t) - \frac{\kappa}{2} m_q(t)\,,\\ \dot{m}_p(t) &= -g m_y(t) + \delta m_q(t) - \frac{\kappa}{2} m_p(t)\,.\end{aligned} \tag{8}$$

A value of m_q or m_p different from zero witnesses a macroscopic occupation of the bosonic mode i.e. a superradiant phase [35]. Furthermore, the macroscopic quantity m_z describes the magnetization in z-direction and is therefore a suitable order parameter. The non-linear differential equations for the scalar functions $m_a(t)$, $m_q(t)$ and $m_p(t)$ describe the dynamics of the system and are thus basis for the subsequent analysis and characterization of the system.

In fact, for the model at hand, the mean-field equations are exact in the thermodynamic limit, as it is proven in Appendix A. There it is shown that

$$\lim_{N\to\infty} \left\langle m_a^N \right\rangle_t - m_a(t) = 0 = \lim_{N\to\infty} \left\langle \alpha^N \right\rangle_t - \alpha(t)\,,$$

with the time-evolved expectation value $\langle \bullet \rangle_t = \langle \exp\left(t\mathcal{L}^*\left[\bullet\right]\right)\rangle$. The exactness of the quadrature mean-field operators of the cavity light mode

$$\lim_{N\to\infty} \left\langle m_q^N \right\rangle_t - m_q(t) = 0 = \lim_{N\to\infty} \left\langle m_p^N \right\rangle_t - m_p(t)\,,$$

thus follows by their definition in terms of the bosonic creation and annihilation operators [see Eq. (6)].

3.2. Stationary phase

By solving the mean-field equations [Eq. (8)] numerically we found that for detunings different from zero the long-time dynamics of the system is always characterized by a stationary state. Therefore, we focus on the case of a laser frequency resonant with the cavity mode and the atom energy splitting (i.e $\delta = \Delta = 0$). To simplify the analysis, we consider that the initial state of the system is chosen such that $m_x(0) = m_q(0) = m_p(0) = 0$. Therefore, m_q and m_x are zero for all times and together with $\delta = \Delta = 0$ the mean-field equations reduce to

$$\begin{aligned}\dot{m}_y(t) &= -2\Omega m_z(t) - \sqrt{2} g m_p(t) m_z(t)\,,\\ \dot{m}_z(t) &= 2\Omega m_y(t) + \sqrt{2} g m_p(t) m_y(t)\,,\\ \dot{m}_p(t) &= -g m_y(t) - \frac{\kappa}{2} m_p(t)\,.\end{aligned} \tag{9}$$

These mean-field equations preserve the norm of the magnetization vector $\boldsymbol{m}_S(t) = (m_x(t), m_y(t), m_z(t))^T$, since

$$\frac{\mathrm{d}}{\mathrm{d}t}||\boldsymbol{m}_S(t)|| = \frac{m_x(t)\dot{m}_x(t) + m_y(t)\dot{m}_y(t) + m_z(t)\dot{m}_z(t)}{||\boldsymbol{m}(t)||} = 0\,.$$

The initial state of the atoms is chosen such that $||\boldsymbol{m}_S(0)||^2 = m_y(0)^2 + m_z(0)^2 = \frac{1}{2}$. In order to find a stationary state, we set the mean-field equations to zero and use that $||\boldsymbol{m}_S(t)||^2 = \frac{1}{2}\,, \forall t$

for the chosen initial state. The stationary state of the system is thus given by

$$m_y^* = \frac{1}{\sqrt{2}}\left(\frac{g_c/\kappa}{g/\kappa}\right)^2, \qquad m_z^* = \pm\frac{1}{\sqrt{2}}\sqrt{1-\left(\frac{g_c/\kappa}{g/\kappa}\right)^4} \qquad \text{and} \qquad m_p^* = -\frac{\sqrt{2}(g_c/\kappa)^2}{g/\kappa}, \tag{10}$$

with the critical coupling $g_c/\kappa = \sqrt{\Omega/\kappa}$. A stability analysis shows that the relevant dynamically stable solution in the stationary phase is the one with the minus sign. A detailed calculation is provided in the Appendix B. For couplings larger than the critical one, the stable solution is physical whereas for smaller couplings the solution is unphysical which can be seen from m_z^* becoming complex. The quantity m_z^* represents the macroscopic magnetization of the spin-ensemble in z-direction and hence this quantity should be real-valued. However, for $g < g_c$ this quantity has a non-vanishing imaginary part and, for this reason, the stationary solution is unphysical. The fact that for $g < g_c$ there is no acceptable stationary solution indicates that the system cannot approach any stationary time-invariant behavior for long times in this parameter regime. It must thus display persistent oscillations.

Additionally, the stationary solution shows that the associated state of the bosonic mode is a coherent state $|\beta\rangle$, with $d\,|\beta\rangle = \beta\,|\beta\rangle$, such that

$$m_q^* = \lim_{N\to\infty}\left\langle m_q^N\right\rangle_\beta = \lim_{N\to\infty}\frac{\sqrt{2}}{\sqrt{N}}\mathrm{Im}(\beta) = 0 \quad \text{and} \quad m_p^* = \lim_{N\to\infty}\left\langle m_p^N\right\rangle_\beta = \lim_{N\to\infty}\frac{\sqrt{2}}{\sqrt{N}}\mathrm{Re}(\beta) \neq 0\,.$$

For this reason, the bosonic mode is macroscopically occupied in the stationary phase of the system which can be seen from the expectation value of the number operator $\langle n\rangle_\beta = \langle\beta|d^\dagger d|\beta\rangle = |\beta|^2 = \mathrm{Re}^2(\beta) + \mathrm{Im}^2(\beta) \propto N$.

3.3. Time-crystal phase and nonequilibrium phase transition

We now want to identify and characterize the nonequilibrium phase transition from the stationary to the time-crystal phase. As we saw above, the time-crystal phase is associated with persistent oscillations of the mean-field variables. In general, the time-integrated value $\overline{\gamma}(t) = \frac{1}{t}\int_0^t \mathrm{d}s\,\gamma(s)$, can be used to see the overall trend of an oscillating quantity $\gamma(t)$. Hence, the time-integrated quantity $\overline{m}_z$ allows one to draw a phase diagram which looks similar to that for phase transitions between stationary phases. Numerical results [see Fig. 2] show that the phase transition from the stationary regime to the time-crystal regime can also occur for couplings larger than the critical coupling. Due to the stability of the stationary solution in this regime, this indicates the emergence of a coexistence region where the stationary phase and the time-crystal one are possible. These are approached according to the specific chosen initial condition.

In order to investigate the coexistence of the two phases, a quantity able to distinguish between the two different dynamical regimes of the system for long times is needed. The time-variance of the magnetization provides information on the behavior of the system, since this quantity is zero for a stationary value while it assumes a finite value for an oscillating state. Therefore, the variance

$$\sigma_c = \sqrt{\frac{1}{N_I}\sum_{i\in I}\left(m_c(t_i) - \overline{m}_c\right)^2}\,,$$

with $c = y, z, p$ and I being an interval for long times, is useful to distinguish between the two phases. To solve the mean-field equations numerically, an initial state is necessary. As before, we

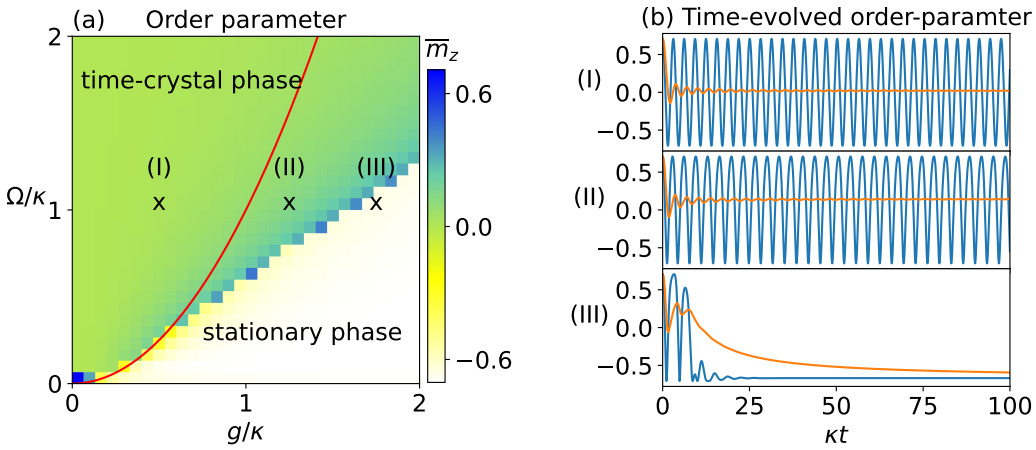

FIG. 2. **Mean-field phase diagram. (a)** Time-averaged value of the magnetization in z-direction for large times as a function of the rescaled coupling g/κ and the driving of the atoms Ω/κ for the initial state of the system $m_y(0) = 0$ and $m_z(0) = \frac{1}{\sqrt{2}}$. The red line indicates where the stationary solution of the mean-field equations becomes unphysical and the phase transition is expected. **(b)** Time-evolution of the magnetization in z-direction $m_z(t)$ (blue line) and corresponding time-integrated value $\overline{m}_z(t)$ (orange line). The driving and the coupling correspond to the values indicated in (a) by the cross ($\Omega/\kappa = 1$ and (I) $g/\kappa = 0.5$, (II) $g/\kappa = 1.25$ and (III) $g/\kappa = 1.75$).

want to restrict ourselves to the initial states $m_x(0) = m_q(0) = 0$ and $||\boldsymbol{m}_S(0)||^2 = 1/2$. Therefore, there are two free parameters $\theta(0)$, with $m_y(0) = \sin(\theta(0))/\sqrt{2}$ and $m_z(0) = \cos(\theta(0))/\sqrt{2}$, where $\theta(0) \in [0, 2\pi)$, and $m_p(0)$. To better explore the extension of the coexistence region, values $m_p(0) \neq 0$ are now allowed. Nevertheless, the assumption $m_q(0) = 0$ is, due to the fact that the state of the cavity is a coherent state, still achievable. The three entries of the vector $(m_y(t), m_z(t), m_p(t))^T$ evolve in the corresponding three-dimensional space on the surface of a cylinder with radius one-half due to the constraint $m_y(t)^2 + m_z(t)^2 = \frac{1}{2}\,, \forall t$. For this reason, the ansatz

$$\begin{aligned} m_y(t) &= \cos(\theta(t))m_y(0) + \sin(\theta(t))m_z(0)\,, \quad \text{with} \quad \dot{m}_y(t) = \dot{\theta}(t)m_z(t)\,, \\ m_z(t) &= \cos(\theta(t))m_z(0) - \sin(\theta(t))m_y(0)\,, \quad \text{with} \quad \dot{m}_z(t) = -\dot{\theta}(t)m_y(t)\,, \end{aligned} \tag{11}$$

with a general time-dependent scalar function $\theta(t)$, reflects the structure of the mean-field equations [Eq. (9)]. The three-dimensional system can be shaped into a two-dimensional form where the magnetization vector evolves in the θ-m_p plane. In the coexistence regime the system approaches for some initial values $\theta(0)$ and $m_p(0)$ the stationary state given by $(m_y^*, m_z^*, m_p^*)^T$ and for others it enters for long times the limit cycle [see Fig. 3]. To understand whether there is coexistence the dynamical parameters g and Ω are fixed and the initial values $\theta(0)$ and $m_p(0)$ are varied. If there is a jump of σ_c as a function of the initial values $\theta(0)$ and $m_p(0)$ one can conclude that the system ends up for certain initial conditions in the stationary phase while for others in the time-crystal one. The size of such a discontinuity is measured by $\delta\sigma_c$, the maximal gradient within the values of σ_c for different initial conditions. Therefore, $\delta\sigma_c$ indicates the coexistence of the phases. As depicted in Fig. 4(a), there are couplings g/κ and drivings Ω/κ where a jump of σ_c occur. For this reason there is coexistence of the two phases for a broad range of dynamical parameters. The coexistence phase is located between the purely time-crystal and the purely stationary phase. For the latter two phases the state of the system for long times is solely determined by the values of the dynamical parameters and is thus independent from the

initial conditions. We now want to investigate the question how the coexistence phase influences the transition between the two phases.

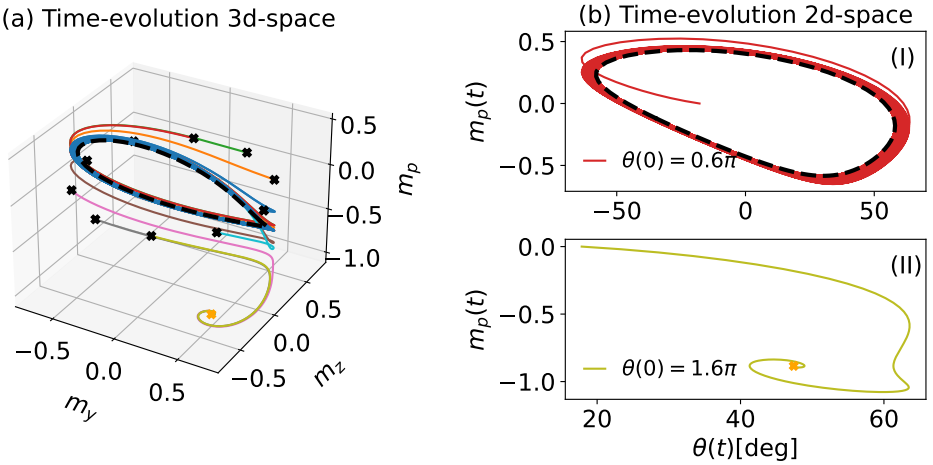

FIG. 3. **Coexistence of the time-crystal and of the stationary state. (a)** Time-evolution of the magnetization vector $(m_y(t), m_z(t), m_p(t))^T$ in the three dimensional space $(m_y, m_z, m_p)^T$ for different initial values of $\theta(0)$ and a fixed value $m_p(0) = 0$. The coupling and the coherent driving are fixed to the values $\Omega/\kappa = 0.5$ and $g/\kappa = 0.8$. The analytical stationary solution in Eq. (10) is highlighted by the orange star. The limit cycle is indicated by the dashed black line. The black crosses show the initial values of the magnetizations in the m_y-m_z-plane. **(b)** Time-evolution of the magnetization vector $(m_y(t), m_z(t), m_p(t))^T$ in the two dimensional space $(\theta, m_p)^T$. The coupling and the coherent driving are fixed to the values $\Omega/\kappa = 0.5$ and $g/\kappa = 0.8$. (I) Limit cycle: The limit cycle is indicated by the dashed black line. (II) Stationary state: The analytical stationary solution in Eq. (10) is highlighted by the orange star.

In a recent work, it was analytically shown that the boundary time-crystal model features a (continuous) second-order phase transition [8, 9]. However, in the present model the N two-level atoms are coupled to an optical cavity which results in the richer phase diagram shown in Fig. 4(a). The phase transition is studied for fixed initial conditions and varying parameters g/κ and Ω/κ. As we have seen in Fig. 2, the phase transition does not necessarily occur on the analytical transition line, i.e. the critical point of the stationary solution. The transition from the time-crystal to the stationary phase can occur for parameters far away from the analytical transition line inside the stationary phase. This behavior corresponds to the emergence of a coexistence regime. We see from Eq. (10) that the magnetization in z-direction in the stationary phase increases towards the analytical transition line and is zero at the critical point. However, due to the possibility of having phase transitions away from the analytical transition line the value m_z^* is not necessarily zero at the point of the phase transition. Therefore, the order parameter $\overline{m}_z$, see Fig. 4b(II), jumps and a first-order phase transition is witnessed. The numerical results [Fig. 4(a)] however show that there is no coexistence for small values of g/κ and Ω/κ. The system changes its phase for all initial conditions on the analytical transition line. The order parameter $\overline{m}_z$ changes continuously on this line and therefore a second-order phase transition occurs [Fig. 4b(I)]. Thus, there is a direct connection between the emergence of the coexistence regime and the change from a second-order to a first-order phase transition.

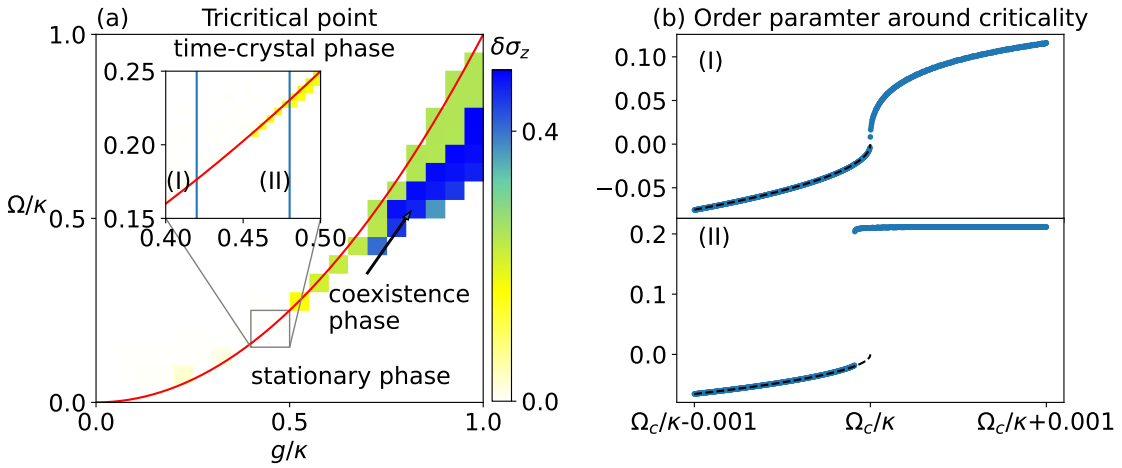

FIG. 4. **First-order and second-order time-crystal phase transition. (a)** Coexistence of the stationary and time-crystal phase measured by the quantity $\delta\sigma_z$ for different values of the coupling and the coherent driving. The red line indicates where the analytical stationary solution becomes unphysical. **(b)** Time-integrated value $\overline{m}_z$ in the long-time limit for a fixed value of the coupling ((I)$g/\kappa = 0.42$, (II)$g/\kappa = 0.48$) in the vicinity of the corresponding critical driving $\Omega_c/\kappa = (g/\kappa)^2$. The black dashed line corresponds to m_z^*, the stationary solution of the magnetization in z-direction in the regime $\Omega/\kappa < \Omega_c/\kappa$. The initial value of the system is fixed to $\theta(0) = 0$ and $m_p(0) = 0$.

4. Fluctuations and correlations

In the previous section, we have determined the long-time behavior of the order parameters and characterized the main features of the phase diagram of the considered system. In the following, the focus is instead on understanding the behavior of correlations both near the phase transition and in the time-crystal regime. In particular, the analysis will concern collective correlations between the atoms and the cavity field. One way to achieve such characterization is by exploiting quantum fluctuation operators [27, 33, 36].

4.1. Quantum fluctuations

The previously discussed mean-field operators converge to multiples of the identity [33] and thus cannot be used to study the behavior of correlations let alone of any genuine quantum feature. Quantum fluctuations, however, defined as the deviation of microscopic quantities from their expectation value, are the relevant quantities to probe quantum correlations in a many-body system [33]. For the considered system consisting of N two-level atoms coupled to an optical cavity we introduce the fluctuation operators

$$F_a^N = \frac{V_a - \langle V_a \rangle}{\sqrt{N}} = \frac{1}{\sqrt{N}} \sum_{k=1}^{N} \left(v_a^{[k]} - \left\langle v_a^{[k]} \right\rangle \right) , \qquad \text{with} \qquad a = x, y, z \tag{12}$$

and

$$F_b^N = b - \langle b \rangle , \qquad \text{with} \qquad b = q, p , \tag{13}$$

to analyze fluctuations of the corresponding mean-field operators. Quantum fluctuations are thus close to the classical ones discussed in the context of central limit theorems. For these classical fluctuations it is known that they can retain correlations. A rather direct connection to classical probability theory can be drawn by identifying the mean-field variables as sample mean

observables and the quantum fluctuations as the corresponding classical random variables. The transfer of the central limit theorem to the collective quantum fluctuations leads to the insight that they form in the thermodynamic limit

$$F_a = \lim_{N\to\infty} F_a^N = \lim_{N\to\infty} \frac{V_a - \langle V_a \rangle}{\sqrt{N}}\,, \qquad \text{with} \qquad a = x, y, z\,, \tag{14}$$

a non-commutative bosonic algebra [25]. Therefore, the commutator of quantum fluctuations is not zero and thus they can retain a quantum character even in the thermodynamic limit [33]. With the commutation relations of the microscopic observables $v_a^{[k]}$ [cf. Eq(3)], it can be shown that the commutator of the collective quantum fluctuations takes the form of a mean-field operator [33]. Since we saw that the the mean-field operators converge in the thermodynamic limit to scalar multiples of the identity, quantum fluctuations behave as bosonic operators in the large N limit. For the fluctuation operators of the cavity mode $F_b^N = b - \langle b \rangle$, where $b = q, p$, it is obvious that they form a bosonic algebra. We use the commutation relation for the rescaled Pauli matrices in Eq. (3) to find an explicit expression for the commutator of the fluctuation operators $[F_a, F_b] = is_{ab}$ with

$$s = \begin{pmatrix} s_S & 0 \\ 0 & s_B \end{pmatrix} = \begin{pmatrix} 0 & \sqrt{2}m_z & -\sqrt{2}m_y & 0 & 0 \\ -\sqrt{2}m_z & 0 & \sqrt{2}m_x & 0 & 0 \\ \sqrt{2}m_y & -\sqrt{2}m_x & 0 & 0 & 0 \\ 0 & 0 & 0 & 0 & 1 \\ 0 & 0 & 0 & -1 & 0 \end{pmatrix}. \tag{15}$$

The matrix s is often referred to as the symplectic matrix of the fluctuation algebra [25, 33].

4.2. Time-evolution of the covariance matrix

To the end of determining the correlations in the two different phases of the system, we introduce the covariance matrix $\Sigma_{ab} = \langle \{F_a, F_b\} \rangle /2$, for the set $\{F_x, F_y, F_z, F_q, F_p\}$ of fluctuation operators. The diagonal elements of the covariance matrix Σ_{aa} represent the susceptibility of the corresponding order parameter m_a. This quantity is crucial to determine the emergence of correlations in the system [9]. The dynamics of the covariance matrix is defined through the time-evolution of the fluctuation operators due to the Lindblad generator in Eq. (2). The covariance matrix of the quantum fluctuations can be rewritten, by using $K_{ab}^N = \left\langle F_a^N F_b^N \right\rangle$, in the following form

$$\Sigma = \lim_{N\to\infty} \frac{K^N + (K^N)^T}{2}\,. \tag{16}$$

A detailed derivation of the different contribution to the time-evolution of the covariance matrix is provided in Appendix C. Nevertheless, the major steps are described in the subsequent discussion. Starting with the Lindblad generator [cf. Eq. (2)], the terms

$$\dot{K}^N = \left\langle \mathcal{L}^N \left[F_a^N F_b^N \right] \right\rangle \tag{17}$$

$$= \left\langle i \left[H, F_a^N \right] F_b^N \right\rangle + \left\langle i F_a^N \left[H, F_b^N \right] \right\rangle + \left\langle \mathcal{D} \left[F_a^N F_b^N \right] \right\rangle\,, \tag{18}$$

contribute to the time-evolution of the matrix K^N. For the first and second term in Eq. (18), the commutator is rewritten in terms of quantum fluctuations and scalars (i.e. expectation values). Together with the fluctuation operator F_b^N these scalar terms do not contribute to

the expectation value since the expectation value of a fluctuation operator alone is zero (i.e. $\langle F_a^N \rangle = 0$). This leads to

$$\lim_{N\to\infty} \left\langle i \left[H, F_a^N\right] F_b^N \right\rangle = (PK)_{ab} \qquad \text{and} \qquad \lim_{N\to\infty} \left\langle i F_a^N \left[H, F_b^N\right] \right\rangle = (KP^T)_{ab}\,,$$

where the explicit form of matrix P can be found in Appendix C. For the dissipative part of the time-evolution the special form of the dissipator is used [36]

$$\mathcal{D}\left[F_a^N F_b^N\right] = F_a^N \mathcal{D}\left[F_b^N\right] + \mathcal{D}\left[F_a^N\right] F_b^N + \kappa \left[a^\dagger, F_a^N\right] \left[F_b^N, a\right]\,, \tag{19}$$

such that

$$\lim_{N\to\infty} \left\langle \mathcal{D}\left[F_a^N F_b^N\right] \right\rangle = (KEs)_{ab} + (sEK)_{ab} - (sE's)_{ab}\,. \tag{20}$$

The explicit form of E', that can be found in Appendix C, shows that this matrix corresponds to the Kossakowski matrix $C = A + iB$ of the dissipative process. Therefore, the time-evolution of the covariance matrix can be written as follows

$$\dot{\Sigma}(t) = \frac{\dot{K} + (\dot{K})^T}{2} = W(t)\Sigma(t) + \Sigma(t)W^T(t) + s(t)As^T(t)\,, \tag{21}$$

with $W(t) = P(t) + s(t)B$. At this point, it is important to notice that apart from the dependence on the system parameters, the matrices $s(t)$ and $P(t)$ are time-dependent. The time-dependence arises from the dynamics of the mean-field observables and thus the evolution of the covariance matrix also depends on the mean-field equations. Because of the classical character of the mean-field observables, the dynamics of the covariance matrix consists of both a quantum and a classical contribution [37]. As we have seen in the discussion of the phase transition towards the time-crystal phase, the mean-field variables can show persistent oscillations for long times. Therefore, the time-dependence can remain even in the long-time limit.

By construction, quantum fluctuations are characterized by Gaussian states [25, 33]. Furthermore, the time-evolution of the associated covariance matrix Eq. (21) has the structure of a bosonic Gaussian quantum channel. The latter preserves the Gaussian character of quantum fluctuations at all times [38]. For Gaussian states the entire information about the chosen degrees of freedom is contained in the covariance matrix. Therefore, the covariance matrix is sufficient for the analysis of correlations in the considered system [27].

4.3. Canonical bosonic modes

In order to take a look at the principal components of the covariance matrix, we move to a frame which rotates solidly with the main direction of the atom mean-field operators. As we will see, this will remove the time-dependence from the commutator in Eq. (15) such that the associated quantum fluctuations can be interpreted as proper bosonic operators.

To achieve this, we rewrite the mean-field equations in Eq. (8) as a matrix equation [33]

$$\frac{\mathrm{d}}{\mathrm{d}t}\boldsymbol{m}(t) = D(t)\boldsymbol{m}(t)\,, \tag{22}$$

by introducing the vector representation of the mean-field variables
$\boldsymbol{m}^T(t) = (m_x(t), m_y(t), m_z(t), m_q(t), m_p(t))^T$ and the time-dependent matrix

$$D(t) = \left(\begin{array}{ccc|cc} 0 & \Delta & \sqrt{2}gm_q(t) & 0 & 0 \\ -\Delta & 0 & -2\Omega - \sqrt{2}gm_p(t) & 0 & 0 \\ -\sqrt{2}gm_q(t) & 2\Omega + \sqrt{2}gm_p(t) & 0 & 0 & 0 \\ \hline g & 0 & 0 & \frac{\kappa}{2} & -\delta \\ 0 & -g & 0 & \delta & \frac{\kappa}{2} \end{array}\right)\,. \tag{23}$$

Thus, the solution of this equation is formally given by

$$\boldsymbol{m}(t) = \overrightarrow{\mathcal{T}}\left[\exp\left(\int_0^t \mathrm{d}s D(s)\right)\right]\boldsymbol{m}(0)\,, \tag{24}$$

with the time-ordering operator $\overrightarrow{\mathcal{T}}$. The Dyson-Series gives an explicit expression for the propagator in Eq. (24). To this end, Eq. (24) is separated into the evolution of the mean-field variables of the atoms $\boldsymbol{m}_S(t)$ and the ones of the cavity $\boldsymbol{m}_B(t)$

$$\begin{pmatrix} \dot{\boldsymbol{m}}_S(t) \\ \dot{\boldsymbol{m}}_B(t) \end{pmatrix} = \begin{pmatrix} D_{SS}(t) & 0_{3\times 2} \\ D_{BS}(t) & D_{BB}(t) \end{pmatrix}\begin{pmatrix} \boldsymbol{m}_S(t) \\ \boldsymbol{m}_B(t) \end{pmatrix} = \begin{pmatrix} D_{SS}(t)\boldsymbol{m}_S(t) \\ D_{BS}(t)\boldsymbol{m}_S(t) + D_{BB}(t)\boldsymbol{m}_B(t) \end{pmatrix}.$$

With the time-dependent matrix $D(t)$ recasted in this form the matrix multiplication in the Dyson-Series

$$\overrightarrow{\mathcal{T}}\left[\exp\left(\int_0^t \mathrm{d}s D(s)\right)\right] = \sum_{N=0}^{\infty}\frac{1}{N!}\int_0^t \mathrm{d}s_1 \cdots \int_0^t \mathrm{d}s_N \overrightarrow{\mathcal{T}}\left[D(s_1)\cdot\ldots\cdot D(s_N)\right],$$

is given by

$$\overrightarrow{\mathcal{T}}\left[D(s_1)\cdot\ldots\cdot D(s_N)\right] = \begin{pmatrix} \tilde{D}_{SS} & 0_{3\times 2} \\ \tilde{D}_{BS} & \tilde{D}_{BB} \end{pmatrix},$$

with $\tilde{D}_{SS} = D_{SS}(s_N)\cdot\ldots\cdot D_{SS}(s_1)$. This leads to a propagator of the following form

$$\begin{pmatrix} \boldsymbol{m}_S(t) \\ \boldsymbol{m}_B(t) \end{pmatrix} = \begin{pmatrix} R_{SS}(t) & 0_{3\times 2} \\ R_{BS}(t) & R_{BB}(t) \end{pmatrix}\begin{pmatrix} \boldsymbol{m}_S(0) \\ \boldsymbol{m}_B(0) \end{pmatrix}. \tag{25}$$

The form of this propagator allows one to change into a frame that moves only with the mean-field variables of the atoms $\boldsymbol{m}_S(t)$. In such a reference frame the commutation relations of a two-mode bosonic system

$$\tilde{R}^T(t)s(t)\tilde{R}(t) = \begin{pmatrix} R_{SS}^T(t)s_S(t)R_{SS}(t) & 0 \\ 0 & s_B \end{pmatrix} = \begin{pmatrix} s_S(0) & 0 \\ 0 & s_B \end{pmatrix}, \tag{26}$$

with

$$\tilde{R}(t) = \begin{pmatrix} R_{SS}(t) & 0 \\ 0 & \mathbf{1} \end{pmatrix} \quad \text{and} \quad \boldsymbol{m}_S(0)^T = (m_x(0), m_y(0), m_z(0))^T = \left(0, 0, \frac{1}{\sqrt{2}}\right)^T, \tag{27}$$

are recovered. This specific choice for the initial conditions of the system corresponds to the microscopic state, where all atoms are aligned in z-direction, i.e all atoms are in the excited state.

The time-evolution of the mean-field variables $\boldsymbol{m}_S(t)$ arises from the microscopic dynamics of the rescaled Pauli matrices [33]

$$\frac{\mathrm{d}}{\mathrm{d}t}v_a^{[k]} \overset{a=x,y,z}{=} \mathcal{L}^N\left[v_a^{[k]}\right] = \sum_{\substack{b=x,y,z,q,p \\ c=x,y,z}} m_b^N f_{abc} v_c^{[k]}\,. \tag{28}$$

Only due to this specific order, $D_{SB}(t)$ is equal zero and thus the time-evolution of $\boldsymbol{m}_S(t)$ is solely determined through $D_{SS}(t)$. We verified that the constructed rotation $\tilde{R}(t)$ indeed leads to the standard bosonic commutation relations by explicitly calculating the matrix multiplication $D_{SS}(t)s_S(t)$ and $s_S(t)D_{SS}(t)$ and using the mean-field solutions for $\dot{s}_S(t)$, which shows that

$$\frac{\mathrm{d}}{\mathrm{d}t}\tilde{R}^T(t)s(t)\tilde{R}(t) = R_{SS}^T(t)\left[-D_{SS}(t), s_S(t)\right]R_{SS}(t) + R_{SS}^T(t)\dot{s}_S(t)R_{SS}(t) = 0\,.$$

4.4. Rotating frame

With the rotation defined in Eq. (27) the covariance matrix reads as follows

$$\tilde{\Sigma}(t) = \begin{pmatrix} R_{SS}^T(t)\Sigma_{SS}(t)R_{SS}(t) & R_{SS}^T(t)\Sigma_{SB}(t) \\ \Sigma_{BS}(t)R_{SS}(t) & \Sigma_{BB}(t) \end{pmatrix}.$$

In the calculation of the time-derivative we used that $\frac{\mathrm{d}}{\mathrm{d}t}R_{SS}(t) = D_{SS}(t)R_{SS}(t)$ and $\frac{\mathrm{d}}{\mathrm{d}t}R_{SS}^T(t) = -R_{SS}^T(t)D_{SS}(t)$ such that

$$\dot{\tilde{\Sigma}}(t) = \begin{pmatrix} R_{SS}^T\left(-D_{SS}\Sigma_{SS} + \dot{\Sigma}_{SS} + \Sigma_{SS}D_{SS}\right)R_{SS} & R_{SS}^T\left(-D_{SS}\Sigma_{SB} + \dot{\Sigma}_{SB}\right) \\ \left(\dot{\Sigma}_{BS} + \Sigma_{BS}D_{SS}\right)\Sigma_{BS}R_{SS} & \dot{\Sigma}_{BB} \end{pmatrix}.$$

With Eq. (21) the different entries can be determined to

$$\dot{\tilde{\Sigma}}(t) = Q(t)\tilde{\Sigma}(t) + \tilde{\Sigma}(t)Q^T(t) + s(0)As^T(0)\,, \tag{29}$$

with

$$Q(t) = \begin{pmatrix} 0 & \tilde{P}_{SB}(t) \\ \tilde{P}_{BS}(t) & \tilde{P}_{BB}(t) \end{pmatrix} + s(0)B = \tilde{R}^T(t)P_0(t)\tilde{R}(t) + s(0)B\,,$$

because $P_{SS}(t)$ in Eq. (21) is equal to $D_{SS}(t)$ in Eq. (22). Further, the matrices A and B are not affected by the change of the frame i.e. $A = \tilde{R}^T(t)A\tilde{R}(t)$ and analogously for B. Therefore, the Kossakowski matrix $C = A + iB$ remains the same since the corresponding dissipative process is restricted to the cavity light mode which is by construction not subject to the rotation. The fluctuation operators in the rotating frame are defined as $\left\{\tilde{F}_x, \tilde{F}_y, \tilde{F}_z, \tilde{F}_q, \tilde{F}_p\right\}$. The last two fluctuation operators correspond to the usual quadrature operators of a bosonic mode, in the present case the bosonic mode of the cavity. However, the first two operators $\tilde{F}_x$ and $\tilde{F}_y$ represent in the new reference system the quadrature operators of the collective spin-system and the operator $\tilde{F}_z$ corresponds to a classical variable due to its commutation relation with all other fluctuation operators

$$\left[\tilde{F}_a, \tilde{F}_b\right] = is_{ab}(0) = \begin{pmatrix} 0 & 1 & 0 & 0 & 0 \\ -1 & 0 & 0 & 0 & 0 \\ 0 & 0 & 0 & 0 & 0 \\ 0 & 0 & 0 & 0 & 1 \\ 0 & 0 & 0 & -1 & 0 \end{pmatrix}_{ab}.$$

The structure of the symplectic matrix $s(0)$ is associated with the one of a two mode bosonic system [39], except of the third row and column. Further, the structure of the time-evolution of the covariance matrix in Eq. (29) confirms that the Gaussian character of the quantum fluctuations in the rotated frame $\tilde{F}_a$ is preserved in the course of time. For the later analysis of correlations and entanglement in the system, it is useful to show that the third row and column of the covariance matrix does not contribute to the time-evolution. This results in a reduced description of the system by two sets of quadrature operators and a symplectic matrix in the exact form of a two mode bosonic system

$$s^{\mathrm{r}}(0) = \bigoplus_{k=1}^{2}\eta\,, \qquad \text{with} \qquad \eta = \begin{pmatrix} 0 & 1 \\ -1 & 0 \end{pmatrix}.$$

For the chosen initial state of the atoms (all in the excited state), the expectation value and the variance of the fluctuation operator $\tilde{F}_z$ are zero and consequently the operator itself. The resulting initial covariance matrix has zeros in the third row and column. With Eq. (29) the formal time-evolution of the covariance matrix

$$\tilde{\Sigma}(t) = X_t \Sigma(0) X_t^T - \int_0^t \mathrm{d}u X_t X_u^{-1} s(0) A s(0)^T \left[X_t X_u^{-1}\right]^T , \tag{30}$$

where $\dot{X}_t = Q(t) X_t$, shows that the entries of the third row and column stay zero for all times. To this end, it is helpful to rewrite the propagator X_t in terms of the Dyson series

$$\overrightarrow{\mathcal{T}}\left[\exp\left(\int_0^t \mathrm{d}s Q(s)\right)\right] = \sum_{N=0}^{\infty} \frac{1}{N!} \int_0^t \mathrm{d}s_1 \ldots \int_0^t \mathrm{d}s_N \overrightarrow{\mathcal{T}}\left[Q(s_1) \cdot \ldots \cdot Q(s_N)\right] .$$

The first part of the time-evolution of the covariance matrix is

$$\sum_{N,N'=0}^{\infty} \tfrac{1}{N!N'!} \int_0^t \mathrm{d}s_1 \cdots \int_0^t \mathrm{d}s_N \int_0^t \mathrm{d}s'_1 \cdots \int_0^t \mathrm{d}s'_N \overrightarrow{\mathcal{T}}\left[Q(s_1) \ldots Q(s_N)\right] \Sigma(0) \left(\overrightarrow{\mathcal{T}}\left[Q(s'_1) \ldots Q(s'_N)\right]\right)^T \tag{31}$$

and therefore the third row and column of the matrix multiplication $Q(s)\Sigma(0)Q(s)^T$ should only contain zeros.

To the aim of explicitly performing the matrix multiplication in Eq. (31), the ansatz in Eq. (11) will be used. This ansatz is fully supported by the form of matrix D in Eq. (23) for $\Delta = 0$ and $m_q = 0$. This results in the following explicit form of the matrices

$$\tilde{R}(t) = \begin{pmatrix} 1 & 0 & 0 & 0 & 0 \\ 0 & \cos(\theta) & \sin(\theta) & 0 & 0 \\ 0 & -\sin(\theta) & \cos(\theta) & 0 & 0 \\ 0 & 0 & 0 & 1 & 0 \\ 0 & 0 & 0 & 0 & 1 \end{pmatrix} \quad \text{and} \quad P^*(t) = \begin{pmatrix} 0 & 0 & 0 & g\cos(\theta) & 0 \\ 0 & 0 & 0 & 0 & -g\cos(\theta) \\ 0 & 0 & 0 & 0 & g\sin(\theta) \\ g & 0 & 0 & 0 & -\delta \\ 0 & -g & 0 & \delta & 0 \end{pmatrix} ,$$

which leads to

$$Q(t) = \begin{pmatrix} 0 & 0 & 0 & g\cos(\theta) & 0 \\ 0 & 0 & 0 & 0 & -g \\ 0 & 0 & 0 & 0 & 0 \\ g & 0 & 0 & -\frac{\kappa}{2} & -\delta \\ 0 & -g\cos(\theta) & -g\sin(\theta) & \delta & -\frac{\kappa}{2} \end{pmatrix} ,$$

where the explicit time-dependence of the general function $\theta(t)$ is dropped for a moment. For these specific conditions the matrix $Q(s)\Sigma(0)Q(s)^T$ contains only zeros in the third row and column and as a result the same is true for $X_t\Sigma(0)X_t^T$. Analogously, it is possible to show that the entries in the third row and column of the matrix $X_t X_u^{-1} s(0) A s(0)^T \left[X_t X_u^{-1}\right]^T$ are zero because $s(0)As(0)^T$ fulfills the condition. The calculations above justify the reduction to 4×4-matrices in Eq. (29) and consequently the covariance matrix is of this form as well

$$\tilde{\Sigma}^{\mathrm{r}}(t) = \begin{pmatrix} \tilde{\Sigma}_{xx} & \tilde{\Sigma}_{xy} & \tilde{\Sigma}_{xq} & \tilde{\Sigma}_{xp} \\ \tilde{\Sigma}_{yx} & \tilde{\Sigma}_{yy} & \tilde{\Sigma}_{yq} & \tilde{\Sigma}_{yp} \\ \tilde{\Sigma}_{qx} & \tilde{\Sigma}_{qy} & \tilde{\Sigma}_{qq} & \tilde{\Sigma}_{qp} \\ \tilde{\Sigma}_{px} & \tilde{\Sigma}_{py} & \tilde{\Sigma}_{pq} & \tilde{\Sigma}_{pp} \end{pmatrix} = \begin{pmatrix} \tilde{\Sigma}^{\mathrm{r}}_{SS} & \tilde{\Sigma}^{\mathrm{r}}_{SB} \\ \tilde{\Sigma}^{\mathrm{r}}_{BS} & \tilde{\Sigma}_{BB} \end{pmatrix} . \tag{32}$$

The entries of the third row and column are not relevant to the evolution of the remaining terms of the covariance matrix.

4.5. Dynamical generator

As we will show in the following discussion, it is possible to derive a generator for the dynamics of the fluctuation operators defined in Eqs. (12) and (13). A time-dependent generator in Lindblad form can be found as shown in Ref. [9]. Such a generator provides insight into the dynamical behavior of the fluctuations in the different phases of the system.

The time-evolution of a generic operator $O(t)$ can be written in terms of a propagator acting on the operator at the initial time, $O(t) = \Lambda_t[O]$. Therefore, the derivative of the time-evolved operator can be written as $\Lambda_t \circ \mathcal{W}_t^*[O]$, where $\circ$ denotes the composition of two maps and $\mathcal{W}_t^*$ is, in general, a time-dependent generator. We use the bosonic algebra of fluctuations in reduced form $\left\{\tilde{F}_x, \tilde{F}_y, \tilde{F}_q, \tilde{F}_p\right\}$, where $\left[\tilde{F}_a, \tilde{F}_b\right] = is^{\mathrm{r}}(0)_{ab}$, with $a, b \in \{x, y, q, p\}$, to construct the dynamical generator. The most general form of such a generator is given by

$$\mathcal{W}_t^*[O] = i\left[\tilde{H}^{\mathrm{r}}, O\right] + \sum_{a,b=1}^{4} C_{ab}^{\mathrm{r}}(t)\left(\tilde{F}_a O \tilde{F}_b - \frac{1}{2}\left\{\tilde{F}_a\tilde{F}_b, O\right\}\right), \tag{33}$$

with the Hamiltonian $\tilde{H}^{\mathrm{r}}(t) = \sum_{a,b} \tilde{h}_{ab}^{\mathrm{r}}(t)\tilde{F}_a\tilde{F}_b$ and the dissipative contribution $C^{\mathrm{r}}(t) = A^{\mathrm{r}}(t) + iB^{\mathrm{r}}(t)$ [37]. In order to reconstruct the time-evolution of the covariance matrix in the rotating frame [cf. Eq. (29)] one defines similar to $K_{ab}^N = \left\langle F_a^N F_b^N \right\rangle$ the product of fluctuations $G_{\mu\nu} = \left\langle \tilde{F}_\mu \tilde{F}_\nu \right\rangle$. The time-evolution of the product of fluctuations is according to Eq. (33) given by

$$\begin{aligned}
\mathcal{W}_t^*\left[\tilde{F}_\mu\tilde{F}_\nu\right] &= \sum_{a,b}\left(i\left[\tilde{h}_{ab}^{\mathrm{r}}(t)\tilde{F}_a\tilde{F}_b, \tilde{F}_\mu\tilde{F}_\nu\right] + \frac{C_{ab}^{\mathrm{r}}(t)}{2}\left(\left[\tilde{F}_a, \tilde{F}_\mu\tilde{F}_\nu\right]\tilde{F}_b + \tilde{F}_a\left[\tilde{F}_\mu\tilde{F}_\nu, \tilde{F}_b\right]\right)\right) \\
&= \mathcal{W}_t^*\left[\tilde{F}_\mu\right]\tilde{F}_\nu + \tilde{F}_\mu\mathcal{W}_t^*\left[\tilde{F}_\nu\right] + \sum_{a,b}\frac{C_{ab}(t)}{2}\left[\tilde{F}_a, \tilde{F}_\mu\right]\left[\tilde{F}_\nu, \tilde{F}_b\right],
\end{aligned}$$

with

$$\begin{aligned}
\mathcal{W}_t^*\left[\tilde{F}_\mu\right] &= \sum_{a,b}\left(i\left[\tilde{h}_{ab}^{\mathrm{r}}(t)\tilde{F}_a\tilde{F}_b, \tilde{F}_\mu\right] + \frac{C_{ab}^{\mathrm{r}}(t)}{2}\left(\left[\tilde{F}_a, \tilde{F}_\mu\right]\tilde{F}_b + \tilde{F}_a\left[\tilde{F}_\mu, \tilde{F}_b\right]\right)\right) \\
&= \sum_{a,b}\left(-\tilde{h}_{ab}^{\mathrm{r}}(t)\left(\tilde{F}_a s_{b\mu}^{\mathrm{r}}(0) + s_{a\mu}(0)\tilde{F}_b\right) + \frac{iC_{ab}^{\mathrm{r}}(t)}{2}\left(s_{a\mu}^{\mathrm{r}}(0)\tilde{F}_b + \tilde{F}_a s_{\mu b}(0)\right)\right) \\
&= \sum_{a,b}\left(-\left(\tilde{h}_{ab}^{\mathrm{r}}(t) + \tilde{h}_{ba}^{\mathrm{r}}(t)\right) + i\left(\frac{C_{ab}^{\mathrm{r}}(t) - C_{ba}(t)}{2}\right)\right)s_{a\mu}^{\mathrm{r}}(0)\tilde{F}_b \\
&= -\sum_{a,b}\left(2\mathrm{Re}\left(\tilde{h}_{ab}^{\mathrm{r}}(t)\right) + B_{ab}^{\mathrm{r}}(t)\right)s_{a\mu}^{\mathrm{r}}(0)\tilde{F}_b\,.
\end{aligned}$$

In the last step we have used that

$$\tilde{h}_{ab}^{\mathrm{r}} = \mathrm{Re}\left(\tilde{h}_{ab}^{\mathrm{r}}\right) + i\mathrm{Im}\left(\tilde{h}_{ab}^{\mathrm{r}}\right), \quad \text{where} \quad \mathrm{Re}\left(\tilde{h}_{ab}^{\mathrm{r}}\right) = \mathrm{Re}\left(\tilde{h}_{ba}^{\mathrm{r}}\right) \quad \text{and} \quad \mathrm{Im}\left(\tilde{h}_{ab}^{\mathrm{r}}\right) = -\mathrm{Im}\left(\tilde{h}_{ba}^{\mathrm{r}}\right).$$

The time-derivative of the operator $G = \left\langle \tilde{F}_\mu\tilde{F}_\nu \right\rangle$ is thus given by

$$\dot{G}(t) = s^{\mathrm{r}}(0)\left(2\mathrm{Re}\left(\tilde{H}^{\mathrm{r}}(t)\right) + B^{\mathrm{r}}\right)G(t) + G(t)\left(2\left(\mathrm{Re}\left(\tilde{H}^{\mathrm{r}}(t)\right)\right)^T + B^{\mathrm{r}}\right)s^{\mathrm{r}}(0) + s^{\mathrm{r}}(0)C^{\mathrm{r}}(t)(s^{\mathrm{r}}(0))^T \tag{34}$$

and as a result the equation

$$\dot{\Sigma}^{\mathrm{r}}(t) = s^{\mathrm{r}}(0)\left(2\mathrm{Re}\left(\tilde{H}^{\mathrm{r}}(t)\right) + B^{\mathrm{r}}\right)\Sigma^{\mathrm{r}}(t) + \Sigma^{\mathrm{r}}(t)\left(2\left(\mathrm{Re}\left(\tilde{H}^{\mathrm{r}}(t)\right)\right)^T + B^{\mathrm{r}}\right)s^{\mathrm{r}}(0) + s^{\mathrm{r}}(0)A^{\mathrm{r}}(t)(s^{\mathrm{r}}(0))^T \tag{35}$$

determines the time-evolution of the covariance matrix. The comparison of Eq. (35) with Eq. (29) in the reduced form, gives rise to an explicit expression for the Hamiltonian in Eq. (33)

$$\begin{aligned} 2s^{\mathrm{r}}(0)\mathrm{Re}\left(\tilde{H}^{\mathrm{r}}(t)\right) + s^{\mathrm{r}}(0)B^{\mathrm{r}} &= \tilde{P}_0^{\mathrm{r}}(t) + s^{\mathrm{r}}(0)B^{\mathrm{r}} \\ \iff 2\left(s^{\mathrm{r}}(0)\right)^T s^{\mathrm{r}}(0)\mathrm{Re}\left(\tilde{H}^{\mathrm{r}}(t)\right) &= \left(s^{\mathrm{r}}(0)\right)^T \tilde{P}_0^{\mathrm{r}}(t)\,, \end{aligned}$$

with

$$\mathrm{Re}\left(\tilde{H}^{\mathrm{r}}(t)\right) = \frac{1}{2}((s^{\mathrm{r}}(0))^T\,\tilde{P}_0^{\mathrm{r}}(t)) = \frac{1}{2}\begin{pmatrix} 0 & 0 & 0 & g \\ 0 & 0 & g\cos(\theta) & 0 \\ 0 & g\cos(\theta) & 0 & 0 \\ g & 0 & 0 & 0 \end{pmatrix}, \tag{36}$$

and $\left(s^{\mathrm{r}}(0)\right)^T s^{\mathrm{r}}(0) = \mathbf{1}$. Consequently, the bosonic generator consists of a time-dependent Hamiltonian and a time-independent dissipator. Interestingly, we can recognize the general structure of the considered model in the dynamical generator for the dynamics of the fluctuation operators. For instance, the time-dependent Hamiltonian in Eq. (36) is completely symmetric and treats the fluctuation operators of the spin ensemble and the cavity light mode in the same way. This reflects the structure of the interaction Hamiltonian in Eq. (1), since the exchange of excitations between the two subsystems is symmetric. Further, the dissipative part in Eq. (33) distinguishes between the two sets of fluctuation operators i.e. $\left\{\tilde{F}_x, \tilde{F}_y\right\}$ and $\left\{\tilde{F}_q, \tilde{F}_p\right\}$. This coincides with the fact that we are not accounting for dissipative effects on the atoms but we only considered photon losses from the cavity [cf. Eq. (2)]. Thus, the time-evolution in Eq. (33) is not only consistent with our model, but also reflects its properties.

The long-time dynamics of quantum fluctuations defined through Eq. (33) will be Markovian in the stationary regime due to the convergence of the dynamical generator to a Markov generator. This can be seen from the fact that in this regime $\theta(t)$ will take a constant value given by $\theta = \arccos(\sqrt{2}m_z^*)$ and thus the Hamiltonian becomes time-independent. Whereas, the persistent time-dependence of the generator in the time-crystal phase highlights the non-Markovian character of the quantum fluctuations dynamics in this phase.

4.6. Correlations

4.6.1. Time-evolved covariance matrix

In the stationary regime the matrix $Q^{\mathrm{r}}(t)$ becomes time-independent, since $\cos(\theta(t)) \to \sqrt{2}\cdot m_z^*$. The stationary state of the covariance matrix $\tilde{\Sigma}_*^{\mathrm{r}}$ can be analytically calculated by a vectorization of the matrix equation

$$\begin{aligned} -\left(s(0)As^T(0)\right)^{\mathrm{r}} &= Q^{\mathrm{r}}\tilde{\Sigma}_*^{\mathrm{r}} + \tilde{\Sigma}_*^{\mathrm{r}}\left(Q^{\mathrm{r}}\right)^T \\ \mathrm{vec}\left(-s(0)^{\mathrm{r}}A^{\mathrm{r}}\left(s^{\mathrm{r}}(0)\right)^T\right) &= \left(Q^{\mathrm{r}}\otimes\mathbf{1}_4 + \mathbf{1}_4\otimes Q^{\mathrm{r}}\right)\mathrm{vec}\left(\tilde{\Sigma}_*^{\mathrm{r}}\right), \end{aligned}$$

with the tensor product $\otimes$ and the vectorization of a $m\times n$-matrix M to a $m\cdot n$-vector, by stacking all the columns to one row (i.e. $M_{m,n} \to \left(M_{\bullet,1}^T, \ldots, M_{\bullet,n}^T\right)^T$) [36]. There exists a unique stationary covariance matrix if and only if the matrix $(Q^{\mathrm{r}}\otimes\mathbf{1}_4 + \mathbf{1}_4\otimes Q^{\mathrm{r}})$ is invertible so that

$$\mathrm{vec}\left(\tilde{\Sigma}_*^{\mathrm{r}}\right) = \left(Q^{\mathrm{r}}\otimes\mathbf{1}_4 + \mathbf{1}_4\otimes Q^{\mathrm{r}}\right)^{-1}\mathrm{vec}\left(-s^{\mathrm{r}}(0)A^{\mathrm{r}}\left(s^{\mathrm{r}}(0)\right)^T\right).$$

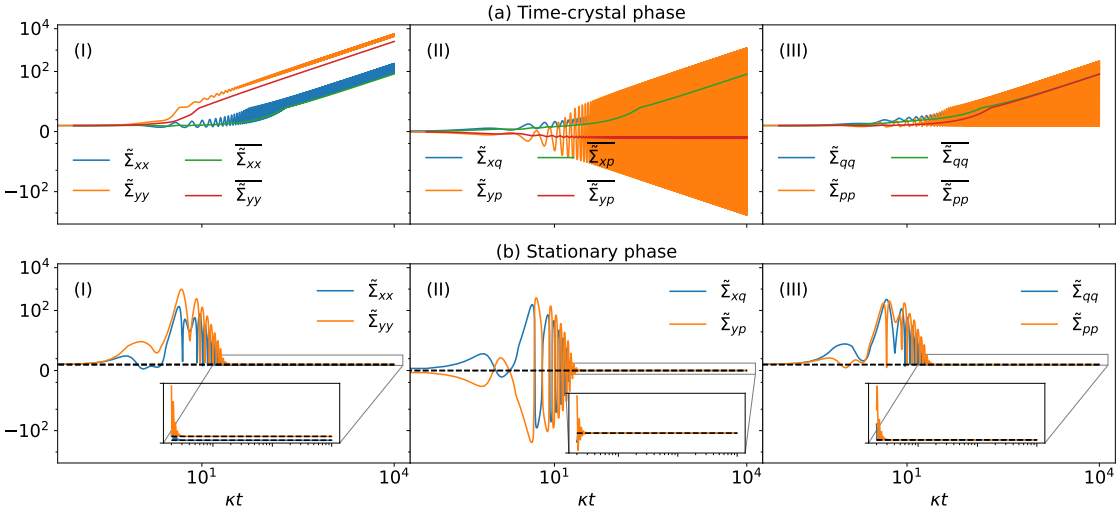

FIG. 5. **Time-evolution of the covariance matrix.** (I), (III) represent the susceptibility for the two-level atoms and the bosonic mode, respectively, and (II) displays correlations between the two subsystems. All the entries $\tilde{\Sigma}_{ab}$ of the covariance matrix that are not illustrated are zero for all times. **(a)** Time-evolution of the covariance matrix in the time-crystal phase for a fixed coupling $g/\kappa = 0.5$ and a fixed driving $\Omega/\kappa = 1$. The time-integrated quantities $\overline{\tilde{\Sigma}}_{ab}$ display the overall trend of the corresponding entries $\tilde{\Sigma}_{ab}$. **(b)** Time-evolution of the covariance matrix in the stationary phase for a fixed coupling $g/\kappa = 0.5$ and a fixed driving $\Omega/\kappa = 1.75$. The dashed lines are the corresponding analytical values from Eq. (37).

The explicit form of the stationary covariance matrix can be calculated analytically to

$$\tilde{\Sigma}_{*}^{\mathrm{r}} = \frac{1}{2}\begin{pmatrix} -\cos(\theta) & 0 & 0 & 0 \\ 0 & -\frac{1}{\cos(\theta)} & 0 & 0 \\ 0 & 0 & 1 & 0 \\ 0 & 0 & 0 & 1 \end{pmatrix}. \tag{37}$$

However, in the time-translation symmetry broken phase, associated with a limit cycle of the mean-field variables, the time-evolution of the covariance matrix, dictated through Eq. (29), is determined numerically. The numerical results for the time-evolution of the covariance matrix indicates that fluctuations increase with time in the entire time-crystal phase [see Fig. 5(a)]. In order to see the emergence of this critical behavior in the two phases of the present model, quantities which measure correlations in the system are analyzed in the following.

4.6.2. Classical correlation and quantum discord

Since we are not only interested in genuine quantum correlations but also in classical ones the one-way classical correlation is introduced. This quantity is a measure for the maximum information about one subsystem that can be gained from the measurement on the other one [36]. The POVM elements $\{\Pi_i\}$, with $\sum_i \Pi_i = \mathbf{1}$, describe the performed measurements. With the definition of the von Neumann entropy $S(\rho) = -\operatorname{Tr}(\rho \log \rho)$ the one-way classical correlation is defined as follows [40]

$$\mathcal{J} = S(\rho_A) - \inf_{\{\Pi_i\}} \sum_i p_i S\left(\frac{\operatorname{Tr}_B(\rho_{AB}\Pi_i)}{p_i}\right). \tag{38}$$

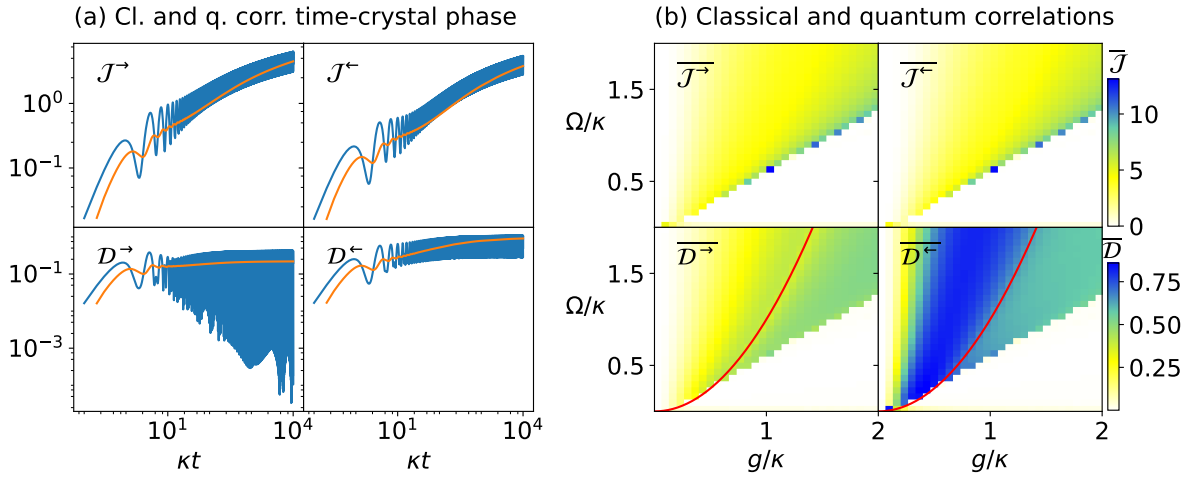

FIG. 6. **Classical correlation and quantum discord.** Classical correlation $\mathcal{J}^{\rightarrow}$ and quantum discord $\mathcal{D}^{\rightarrow}$ for a measurement on the spin ensemble. Classical correlation $\mathcal{J}^{\leftarrow}$ and quantum discord $\mathcal{D}^{\leftarrow}$ for a measurement on the cavity mode. **(a)** The driving is fixed to $\Omega/\kappa = 1$ and the coupling to $g/\kappa = 0.5$. The orange lines are the corresponding time-integrated values. **(b)** Time-integrated value for large times as a function of the driving Ω/κ and the coupling g/κ. The red line indicates where the analytical stationary solution becomes unphysical.

The system is described by the bipartite quantum state ρ_{AB} since it consists of two subsystems. For each subsystem there exists a set of measurement operators $\{\,\Pi_i\,\}$. Applying the measurement Π_i onto the subsystem B results in the state

$$\rho_{A|i} = \mathrm{Tr}_B\left(\frac{\rho_{AB}\Pi_i}{p_i}\right), \qquad \text{with} \qquad p_i = \mathrm{Tr}_{A,B}\left(\rho_{AB}\Pi_i\right),$$

for subsystem A. Basically, one can measure the spin system or the bosonic system which results in two different quantities of the one-way classical correlation labeled by $\mathcal{J}^{\rightarrow}$ and $\mathcal{J}^{\leftarrow}$ respectively.

Another important quantity in the analysis of correlations is the quantum discord

$$\mathcal{D} = I\left(\rho_{ab}\right) - \mathcal{J}, \tag{39}$$

defined through the mutual information $I\left(\rho_{AB}\right) = S\left(\rho_A\right) + S\left(\rho_B\right) - S\left(\rho_{AB}\right)$ and the one-way classical correlation $\mathcal{J}$ [40]. Consequently, there exists a quantum discord $\mathcal{D}^{\rightarrow}$ for a measurement on the spin system and analog one for a measurement on the bosonic system $\mathcal{D}^{\leftarrow}$. The quantum discord measures if separable states, which are typically associated with classically correlated states, still retain a quantum character.

For a two-mode Gaussian state an expression for the one-way classical correlation

$$\mathcal{J}^{\leftarrow} = f(\sqrt{B}) - f(\sqrt{E_{\mathrm{min}}}) \tag{40}$$

and the quantum discord

$$\mathcal{D}^{\leftarrow} = f(\sqrt{B}) - f(\nu_-) - f(\nu_+) + f(\sqrt{E_{\mathrm{min}}}), \tag{41}$$

can be derived in terms of the quantities

$$A = \det(2\tilde{\Sigma}^{\mathrm{r}}_{SS}), \qquad B = \det(2\tilde{\Sigma}_{BB}), \qquad C = \det(2\tilde{\Sigma}^{\mathrm{r}}_{SB}), \qquad D = \det(2\tilde{\Sigma}^{\mathrm{r}}),$$

from the covariance matrix in Eq. (32) [40]. The function f is given by

$$f(x) = \left(\frac{x+1}{2}\right)\log\left(\frac{x+1}{2}\right) - \left(\frac{x-1}{2}\right)\log\left(\frac{x-1}{2}\right),$$

and $E_{\min}$ is defined as

$$E_{\min} = \begin{cases} \frac{2C^2+(B-1)(D-A)+2|C|\sqrt{C^2+(B-1)(D-A)}}{(B-1)^2} & \text{for } (D-AB)^2 \leq (1+B)C^2(A+D), \\ \frac{AB-C^2+D-\sqrt{C^4+(D-AB)^2-2C^2(AB+D)}}{2B} & \text{otherwise}. \end{cases}$$

The quantities ν_- and ν_+ are the symplectic eigenvalues of the matrix $2\tilde{\Sigma}^{\mathrm{r}}$, with $\nu_- < \nu_+$. Williamson theorem [41] states that there exists a transformation S such that $2\tilde{\Sigma}^{\mathrm{r}} = S^T\mathcal{N}S$ with $\mathcal{N} = \mathrm{diag}\,(\nu_1, \nu_1, \nu_2, \nu_2)$. For a measurement on the spin system, $\mathcal{J}^{\rightarrow}$ and $\mathcal{D}^{\rightarrow}$ are as-well defined through Eqs. (40) and (41) just by changing the definition of A and B (i.e. $A = \det(2\tilde{\Sigma}_{BB})$ and $B = \det(2\tilde{\Sigma}^{\mathrm{r}}_{SS})$).

From the stationary solution of the covariance matrix in Eq. (37), it follows that the classical correlation as well as the quantum discord are zero in this phase. This is substantiated by the numerical results in Fig. 6(b). Whereas, the classical correlation and the quantum discord show oscillations in the time-crystalline phase [see Fig. 6(a)]. We introduce the time-integrated values for these quantities analog to the one for the magnetization in z-direction in order to see their overall trend. Interestingly, on the one hand the classical correlation increases indefinitely with time, on the other hand the quantum discord converges to a fixed value. Therefore, the time-integrated values depicted in Fig. 6(b) show that the built-up of classical correlations in the system is larger near the phase transition. Remarkably, the quantum discord $\mathcal{D}^{\leftarrow}$ does not reach its maximal value at the actual phase transition, but for values smaller then the analytical prediction for the phase transition. Further, both the classical correlation and the quantum discord are non-zero not only in the vicinity of the phase transition but in the entire time-crystal phase.

4.6.3. Entanglement

In order to probe the presence of collective entanglement between the atoms and the cavity light field, we investigate a measure of entanglement for the covariance matrix. Since we are dealing with a bipartite system the logarithmic negativity measures whether the states of the two subsystems are separable and thus witnesses entanglement. The logarithmic negativity is defined as

$$\mathcal{E}_{\mathcal{N}} = \max\left(0, -\log\left(\tilde{\nu}_-\right)\right),$$

with the smallest symplectic eigenvalue of the partially transposed covariance matrix $\tilde{\nu}_-$. The partial transposition of the covariance matrix corresponds to changing the sign of one of the two fluctuation operators $\tilde{F}_q, \tilde{F}_p$ (i.e $C \rightarrow -C$).

The numerical results [see Fig. 7(a)] highlight the fact that the time-integrated value of the logarithmic negativity converges in the time-crystal phase to a fixed value. From the stationary covariance matrix in Eq. (37) it is obvious that the entanglement is zero in this phase, which is supported by numerical results [see Fig. 7(b)]. The phase diagram of the time-integrated value of the logarithmic negativity in Fig. 7(b) displays that the time-crystal phase is as a whole a critical phase with diverging fluctuations and strong quantum character.

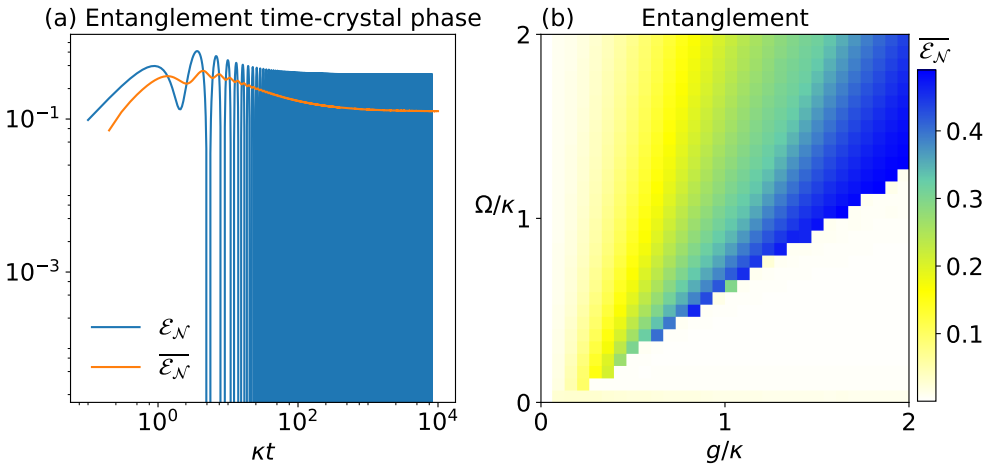

FIG. 7. **Bipartite entanglement.** Logarithmic negativity $\mathcal{E}_\mathcal{N}$ as a measure of entanglement between the two-level atoms and the cavity mode. **(a)** The driving is fixed to $\Omega/\kappa = 1$ and the coupling to $g/\kappa = 0.5$. The orange line is the corresponding time-integrated value. **(b)** Time-integrated logarithmic negativity for large times as a function of the driving Ω/κ and the coupling g/κ.

4.6.4. Squeezing

The uncertainty principle, one of the most fundamental concepts in quantum physics, states that the product of the variance of two non-commutating observables has a lower bound. However, there are so-called squeezed states for which the variance of one of the two observables is smaller than this lower bound. Squeezing of a quantum state indicates the existence of correlations in the system [42]. In the frame rotating with the spin mean-field observables, the system consists of two different sets of quadrature operators: the fluctuation operators of the original bosonic cavity mode and the fluctuation operators of the collective spin in x-and y-direction. With the squeezing parameter ξ there exists a measure for correlations within each subsystem. In general, the squeezing parameter is defined by $\xi = 2 \cdot \min(\phi_1, \phi_2)$, where ϕ_1 and ϕ_2 are the eigenvalues of the submatrices associated with the two subsystems [36]. In this framework, spin squeezing is indicated by a squeezing parameter $\xi_S < 1$ calculated with the submatrix $\tilde{\Sigma}^{\mathrm{r}}_{SS}$. With the submatrix $\tilde{\Sigma}_{BB}$ the boson squeezing parameter ξ_B can be calculated.

The squeezing parameter is set to one for values larger than one, since we focus on the question whether squeezing takes place. Moreover, a squeezed state of the system is only physically relevant if it is squeezed for a certain amount of time. Thus, the modified squeezing parameter $\tilde{\xi}$ is introduced to exclude oscillations of the squeezing parameter from the analysis. Due to the diagonal form of the submatrices $\tilde{\Sigma}_{BB}$ and $\tilde{\Sigma}^{\mathrm{r}}_{SS}$ the corresponding squeezing parameters can be easily read off. Therefore, the numerical results for the time-evolution of the susceptibility $\tilde{\Sigma}_{aa}$, with $a \in \{x, y, q, p\}$, illustrated in Fig. 5(a), show that there is no relevant squeezing for the spin subsystem as well as for the bosonic cavity mode in the time-crystal phase. The stationary covariance matrix in Eq. (37) shows that correlations in the spin subsystem are expected in the stationary phase. The numerical results displayed in Fig. 8 substantiate this claim.

In the stationary phase the squeezing parameter for the spin subsystem is given by $\tilde{\xi}_s = -\sqrt{2} m^*_z$. Thus, the squeezing parameter should go to zero if the coupling g/κ approaches the critical coupling g_c/κ [cf. Eq. (10)]. As previously discussed, this is only possible where the transition from the stationary to the time-crystal phase occurs on the analytical transition line. Therefore,

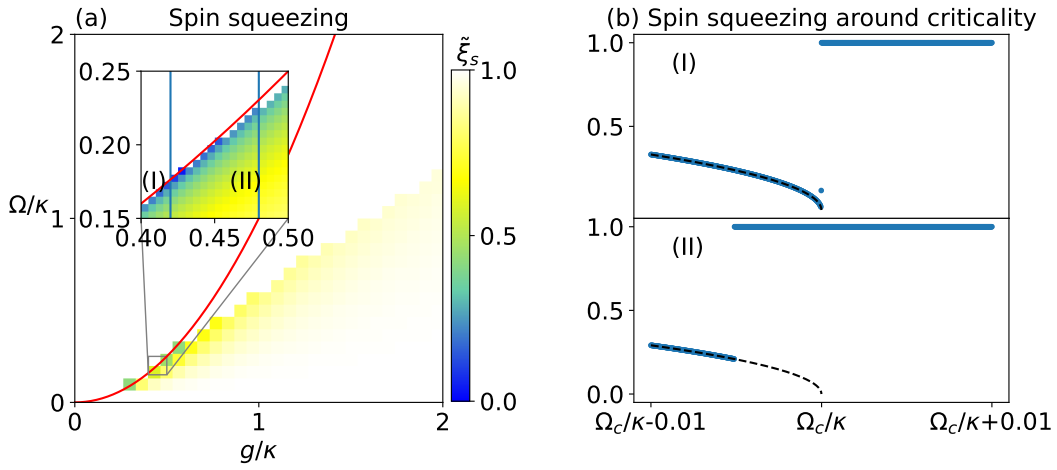

FIG. 8. **Spin squeezing.** Spin squeezing parameter $\tilde{\xi}_s$ as a measure for correlations in the spin ensemble. **(a)** Spin squeezing parameter $\tilde{\xi}_s$ for large times as a function of the driving Ω/κ and the coupling g/κ. The red line indicates where the analytical stationary solution becomes unphysical. **(b)** Spin squeezing parameter $\tilde{\xi}_s$ for large times for a fixed value of the coupling ((I)$g/\kappa = 0.42$, (II)$g/\kappa = 0.48$) in the vicinity of the corresponding critical driving $\Omega_c/\kappa = (g/\kappa)^2$. The black dashed line corresponds to the analytical solution of $\tilde{\xi}_s$ from Eq. (37) in the stationary regime $\Omega/\kappa < \Omega_c/\kappa$.

the spin squeezing parameter should prove as well the change from a first-order to a second-order phase transition for small values of g/κ and Ω/κ. This expected behavior can actually be observed [see Fig. 8(b)]. This result shows that the large spin-squeezing observed for the boundary time-crystal model [9] occurs in the considered driven-dissipative spin-boson model only for the continuous second-order phase transition.

5. Conclusion and outlook

In this thesis, we have analyzed and characterized the phase transition from the stationary to the time-crystal phase as well as correlations for a model consisting of an atom ensemble coupled to a cavity. It was possible to verify that a set of nonlinear differential equations governs the dynamical behavior of the order parameter for a large number of atoms. The behavior of the order parameter at criticality further illustrates the change of the phase transition. The analysis of correlations in the system underlines that fluctuations are unbounded in the time-crystal phase. In the stationary regime, the subsystems are uncorrelated and strong correlations are only witnessed in the atom ensemble in the form of spin squeezing. However, as the system enters the time-crystal phase the spin system is correlated with the cavity mode. Moreover, the classical and quantum correlations are not restricted to a parameter regime near the phase transition. Consequently, this indicates that the time-crystal phase is as a whole a critical phase. Interestingly, the change in the nature of the phase transition, dependent on the coupling between the two subsystems and the driving, is as well reflected in the evolution of correlations in the system such as the spin squeezing. Additionally, we found entanglement in the time-crystal phase.

We introduced quantum fluctuations towards a better understanding of correlations in the time-crystal phase, since the corresponding covariance matrix forms a starting point for this analysis. This work provides a framework in which fluctuations of a coupled atom system which

evolve with time can be brought into a canonical bosonic form by going into a rotated frame. The constraints for this were discussed and derived from the microscopic picture. The breaking of the time-translation symmetry resulting in a non-Markovian evolution of the system found before [9], was underlined in the considered model. In fact, a time-dependent generator with a coherent and a dissipative contribution for the quantum fluctuations was derived.

Furthermore, the results give rise to the question of possible applications of the time-crystal phase in the field of quantum information theory. Since entangled states are extremely relevant for quantum information theory, the entanglement of the spin ensemble and the cavity mode inside this many-body phase could be of interest. Nevertheless, apart from entangled states, the quantum discord could be used for quantum-enhanced measurements [36, 43]. Further, the squeezing of the spin ensemble could be of interest for quantum metrology. However, different effects have to be taken into account for the experimental application. In the presented setup local spin-decay was neglected although this is certainly a relevant process in experiments. In addition, in experimental setups, similar to the one studied here, the number of atoms inside the cavity is clearly finite [34]. Due to these two effects, it is assumed that the stationary and the time-crystal phase appear as metastable states in the dynamical transition regime towards a new unique stationary state [23, 44].

References

[1]R. H. Dicke, 'Coherence in spontaneous radiation processes', Phys. Rev. **93**, 99–110 (1954).

[2]K. Hepp and E. H. Lieb, 'Equilibrium statistical mechanics of matter interacting with the quantized radiation field', Phys. Rev. A **8**, 2517–2525 (1973).

[3]M. Tavis and F. W. Cummings, 'Exact solution for an N-molecule—radiation-field hamiltonian', Phys. Rev. **170**, 379–384 (1968).

[4]E. Jaynes and F. Cummings, 'Comparison of quantum and semiclassical radiation theories with application to the beam maser', Proceedings of the IEEE **51**, 89–109 (1963).

[5]F. Dimer, B. Estienne, A. S. Parkins and H. J. Carmichael, 'Proposed realization of the dicke-model quantum phase transition in an optical cavity qed system', Phys. Rev. A **75**, 013804 (2007).

[6]P. Kirton and J. Keeling, 'Superradiant and lasing states in driven-dissipative dicke models', New Journal of Physics **20**, 015009 (2018).

[7]B. Buča, J. Tindall and D. Jaksch, 'Non-stationary coherent quantum many-body dynamics through dissipation', Nature Communications **10**, 1730 (2019).

[8]F. Iemini, A. Russomanno, J. Keeling, M. Schirò, M. Dalmonte and R. Fazio, 'Boundary time crystals', Phys. Rev. Lett. **121**, 035301 (2018).

[9]F. Carollo and I. Lesanovsky, 'Exact solution of a boundary time-crystal phase transition: time-translation symmetry breaking and non-markovian dynamics of correlations', Phys. Rev. A **105**, L040202 (2022).

[10]F. Wilczek, 'Quantum time crystals', Phys. Rev. Lett. **109**, 160401 (2012).

[11]P. Bruno, 'Impossibility of spontaneously rotating time crystals: a no-go theorem', Phys. Rev. Lett. **111**, 070402 (2013).

[12]H. Watanabe and M. Oshikawa, 'Absence of quantum time crystals', Phys. Rev. Lett. **114**, 251603 (2015).

[13]L. Guo and P. Liang, 'Condensed matter physics in time crystals', New Journal of Physics **22**, 075003 (2020).

[14]N. Y. Yao, A. C. Potter, I.-D. Potirniche and A. Vishwanath, 'Discrete time crystals: rigidity, criticality, and realizations', Phys. Rev. Lett. **118**, 030401 (2017).

[15]V. Khemani, A. Lazarides, R. Moessner and S. L. Sondhi, 'Phase structure of driven quantum systems', Phys. Rev. Lett. **116**, 250401 (2016).

[16]R. Hurtado-Gutiérrez, F. Carollo, C. Pérez-Espigares and P. I. Hurtado, 'Building continuous time crystals from rare events', Phys. Rev. Lett. **125**, 160601 (2020).

[17]F. M. Gambetta, F. Carollo, M. Marcuzzi, J. P. Garrahan and I. Lesanovsky, 'Discrete time crystals in the absence of manifest symmetries or disorder in open quantum systems', Phys. Rev. Lett. **122**, 015701 (2019).

[18]N. Y. Yao, C. Nayak, L. Balents and M. P. Zaletel, 'Classical discrete time crystals', Nature Physics **16**, 438–447 (2020).

[19]S. Choi, J. Choi, R. Landig, G. Kucsko, H. Zhou, J. Isoya, F. Jelezko, S. Onoda, H. Sumiya, V. Khemani, C. von Keyserlingk, N. Y. Yao, E. Demler and M. D. Lukin, 'Observation of discrete time-crystalline order in a disordered dipolar many-body system', Nature **543**, 221–225 (2017).

[20]N. Dogra, M. Landini, K. Kroeger, L. Hruby, T. Donner and T. Esslinger, 'Dissipation-induced structural instability and chiral dynamics in a quantum gas', Science **366**, 1496–1499 (2019).

[21]B. Buča and D. Jaksch, 'Dissipation induced nonstationarity in a quantum gas', Phys. Rev. Lett. **123**, 260401 (2019).

[22]F. Carollo, K. Brandner and I. Lesanovsky, 'Nonequilibrium many-body quantum engine driven by time-translation symmetry breaking', Phys. Rev. Lett. **125**, 240602 (2020).

[23]G. Buonaiuto, F. Carollo, B. Olmos and I. Lesanovsky, 'Dynamical phases and quantum correlations in an emitter-waveguide system with feedback', Phys. Rev. Lett. **127**, 133601 (2021).

[24]L. F. d. Prazeres, L. d. S. Souza and F. Iemini, 'Boundary time crystals in collective d-level systems', Phys. Rev. B **103**, 184308 (2021).

[25]A. F. Verbeure, *Many-body boson systems: half a century later* (Springer, London, 2011).

[26]D. Goderis, A. Verbeure and P. Vets, 'Non-commutative central limits', Probability Theory and Related Fields **82**, 527–544 (1989).

[27]F. Benatti, F. Carollo and R. Floreanini, 'Environment induced entanglement in many-body mesoscopic systems', Physics Letters A **378**, 1700–1703 (2014).

[28]F. Benatti, F. Carollo and R. Floreanini, 'Dissipative entanglement of quantum spin fluctuations', Journal of Mathematical Physics **57**, 062208 (2016).

[29]A. C. Lourenço, L. F. d. Prazeres, T. O. Maciel, F. Iemini and E. I. Duzzioni, 'Genuine multipartite correlations in a boundary time crystal', Phys. Rev. B **105**, 134422 (2022).

[30]C. Hamsen, K. N. Tolazzi, T. Wilk and G. Rempe, 'Two-photon blockade in an atom-driven cavity qed system', Phys. Rev. Lett. **118**, 133604 (2017).

[31]H. Breuer and F. Petruccione, *The theory of open quantum systems* (Oxford University Press, Oxford New York, 2002).

[32]V. Gorini, A. Kossakowski and E. C. G. Sudarshan, 'Completely positive dynamical semigroups of n-level systems', Journal of Mathematical Physics **17**, 821–825 (1976).

[33]F. Benatti, F. Carollo, R. Floreanini and H. Narnhofer, 'Quantum fluctuations in mesoscopic systems', Journal of Physics A: Mathematical and Theoretical **50**, 423001 (2017).

[34]G. Ferioli, A. Glicenstein, I. Ferrier-Barbut and A. Browaeys, 'Observation of a non-equilibrium superradiant phase transition in free space', `10.48550/ARXIV.2207.10361` (2022).

[35]F. Carollo and I. Lesanovsky, 'Exactness of mean-field equations for open dicke models with an application to pattern retrieval dynamics', Phys. Rev. Lett. **126**, 230601 (2021).

[36]M. Boneberg, I. Lesanovsky and F. Carollo, 'Quantum fluctuations and correlations in open quantum dicke models', Phys. Rev. A **106**, 012212 (2022).

[37]F. Benatti, F. Carollo, R. Floreanini and H. Narnhofer, 'Quantum spin chain dissipative mean-field dynamics', Journal of Physics A: Mathematical and Theoretical **51**, 325001 (2018).

[38]T. Heinosaari, A. S. Holevo and M. M. Wolf, 'The semigroup sturucture of gaussian channels', Quantum Inf. Comput. **10**, 619–635 (2010).

[39]G. Adesso and F. Illuminati, 'Entanglement in continuous-variable systems: recent advances and current perspectives', Journal of Physics A: Mathematical and Theoretical **40**, 7821 (2007).

[40]G. Adesso and A. Datta, 'Quantum versus classical correlations in gaussian states', Phys. Rev. Lett. **105**, 030501 (2010).

[41]J. Williamson, 'On the algebraic problem concerning the normal forms of linear dynamical systems', American Journal of Mathematics **58**, 141–163 (1936).

[42]C. Gross, 'Spin squeezing, entanglement and quantum metrology with bose–einstein condensates', Journal of Physics B: Atomic, Molecular and Optical Physics **45**, 103001 (2012).

[43]D. Braun, G. Adesso, F. Benatti, R. Floreanini, U. Marzolino, M. W. Mitchell and S. Pirandola, 'Quantum-enhanced measurements without entanglement', Rev. Mod. Phys. **90**, 035006 (2018).

[44]A. Kouzelis, K. Macieszczak, J. Minar and I. Lesanovsky, 'Dissipative quantum state preparation and metastability in two-photon micromasers', Phys. Rev. A **101**, 043847 (2020).

A. Proof of the exactness of the mean-field variables

Within the framework provided in the supplemental material of [35] it is possible to show that the mean-field equations

$$\dot{m}_a(t) = \sum_b \left(-2\Omega\varepsilon_{xab} + \Delta\varepsilon_{zab} - g\left(\left(\alpha(t) + \alpha(t)^\dagger\right)\varepsilon_{xab} - i\left(\alpha(t) - \alpha(t)^\dagger\right)\varepsilon_{yab}\right)\right) m_b(t)\,, \tag{42}$$

$$\dot{\alpha}(t) = \frac{ig}{\sqrt{2}}\left(-m_x(t) + im_y(t)\right) + i\delta\alpha(t) - \frac{\kappa}{2}\alpha(t)\,, \tag{43}$$

are exact in the thermodynamic limit i.e

$$\lim_{N\to\infty}\left\langle m_a^N\right\rangle_t - m_a(t) = 0 = \lim_{N\to\infty}\left\langle \alpha^N\right\rangle_t - \alpha(t)\,, \qquad \text{with} \qquad \langle\bullet\rangle_t = \langle\exp\left(t\mathcal{L}^*\left[\bullet\right]\right)\rangle\ .$$

Further, the action of the adjoint Lindblad operator onto the mean-field operators is known

$$\mathcal{L}^*\left[m_a^N\right] = \sum_b \left(-2\Omega\varepsilon_{xab} + \Delta\varepsilon_{zab} - g\left(\left(\alpha^N + (\alpha^N)^\dagger\right)\varepsilon_{xab} - i\left(\alpha^N - (\alpha^N)^\dagger\right)\varepsilon_{yab}\right)\right) m_b^N\,, \tag{44}$$

$$\mathcal{L}^*\left[\alpha^N\right] = \frac{ig}{\sqrt{2}}\left(-m_x^N + im_y^N\right) + i\delta\alpha^N - \frac{\kappa}{2}\alpha^N\,. \tag{45}$$

In a first step a cost function

$$\mathcal{E}_N(t) = \sum_a \left\langle E_a^2\right\rangle_t + \left\langle A^\dagger A + AA^\dagger\right\rangle_t\,,$$

with $E_a = m_a^N - m_a(t)$ and $A = \alpha^N - \alpha(t)$, is defined. Intuitively, this function measures the error, i.e. the number of spins or bosons with a time-evolution different from the one defined by the mean-field equations. Thus, to prove the exactness of the mean-field equations it must be shown that $\lim_{N\to\infty}\mathcal{E}_N(t) = 0$, since in this case the dynamics is fully captured by the mean-field equations. For this purpose Gronwall's Lemma together with the initial condition $\lim_{N\to\infty}\mathcal{E}_N(0) = 0$ is used [35]. The aim is to find a constant C such that $\frac{\mathrm{d}}{\mathrm{d}t}\mathcal{E}_N(t) \le C\mathcal{E}_N(t)$. To this end, the time-derivative of the different parts

$$\frac{\mathrm{d}}{\mathrm{d}t}\mathcal{E}_N(t) = \sum_a \frac{\mathrm{d}}{\mathrm{d}t}\left\langle E_a^2\right\rangle_t + \frac{\mathrm{d}}{\mathrm{d}t}\left\langle A^\dagger A + AA^\dagger\right\rangle_t\,,$$

is calculated and hereby the existence of such a constant C can be shown. In the following proof an initial clustering state, i.e. a state with short-range correlations, is assumed. The proof is separated into finding a constant S for the spin system and a constant B for the bosonic mode.

Spin operators For the spin components the calculation starts with the time-derivative of the corresponding cost function

$$\frac{\mathrm{d}}{\mathrm{d}t}\left\langle(m_a^N - m_a(t))^2\right\rangle_t = \left\langle\mathcal{L}^*\left[(m_a^N - m_a(t))^2\right]\right\rangle_t - 2\dot{m}_a(t)\left\langle m_a^N - m_a(t)\right\rangle_t\,.$$

We make use of the explicit form of the time-evolved expectation value and the knowledge about the structure of the adjoint Lindblad generator acting on the mean-field operators m_a^N [Eq. (44)]. The derivative takes the following form

$$\frac{\mathrm{d}}{\mathrm{d}t}\left\langle(m_a^N - m_a(t))^2\right\rangle_t = D_t^S + \left(D_t^S\right)^* \qquad \text{with} \qquad D_t^S = \left\langle\left(\mathcal{L}^*\left[m_a^N\right] - \dot{m}_a(t)\right)\left(m_a^N - m_a(t)\right)\right\rangle_t\,,$$

and

$$\begin{aligned}\mathcal{L}^*\left[m_a^N\right] - \dot{m}_a(t) = {}& \left(-2\Omega\varepsilon_{xab} + \Delta\varepsilon_{zab}\right)\left(m_b^N - m_b(t)\right)\\ & - g\left(\underbrace{\left(\alpha^N + (\alpha^N)^\dagger\right)m_b^N - \left(\alpha(t) + \alpha(t)^\dagger\right)m_b(t)}_{(C1)}\right)\varepsilon_{xab}\\ & - ig\left(\underbrace{\left(\alpha^N - (\alpha^N)^\dagger\right)m_b^N - \left(\alpha(t) - \alpha(t)^\dagger\right)m_b(t)}_{(C2)}\right)\varepsilon_{yab}\,.\end{aligned}$$

The open index b indicates the summation over it. To proceed further, the aim is to reconstruct differences between the mean-field operators and their scalar version. This can be achieved by adding and subtracting $\left(\alpha(t)+\alpha(t)^\dagger\right) m_b^N$ for $(C1)$ and $\left(\alpha(t)-\alpha(t)^\dagger\right) m_b^N$ for $(C2)$. One ends up with a lengthy expression for D_t^S

$$\begin{aligned}
D_t^S = &(-2\Omega\varepsilon_{xab}+\Delta\varepsilon_{zab})\left\langle\left(m_b^N-m_b(t)\right)\left(m_a^N-m_a(t)\right)\right\rangle_t \\
&-g\Big(\left\langle\left(\alpha^N-\alpha(t)\right)m_b^N\left(m_a^N-m_a(t)\right)\right\rangle_t+\left\langle\left((\alpha^N)^\dagger-\alpha^\dagger(t)\right)m_b^N\left(m_a^N-m_a(t)\right)\right\rangle_t \\
&+\left\langle\left(\alpha^\dagger(t)+\alpha(t)\right)\left(m_b^N-m_b(t)\right)\left(m_a^N-m_a(t)\right)\right\rangle_t\Big)\varepsilon_{xab} \\
&-ig\Big(\left\langle\left(\alpha^N-\alpha(t)\right)m_b^N\left(m_a^N-m_a(t)\right)\right\rangle_t-\left\langle\left((\alpha^N)^\dagger-\alpha^\dagger(t)\right)m_b^N\left(m_a^N-m_a(t)\right)\right\rangle_t \\
&+\left\langle\left(\alpha^\dagger(t)+\alpha(t)\right)\left(m_b^N-m_b(t)\right)\left(m_a^N-m_a(t)\right)\right\rangle_t\Big)\varepsilon_{yab}\,.
\end{aligned}$$

To find the constant S, the modulus of this term is the relevant quantity. With Lemma 1 from the supplemental material of [35] it is possible to find bounds for the different contributions

$$\left|D_t^S\right| \leq \left(6|\Omega|+3|\Delta|+12|g|+3|g|\underbrace{\left(|\alpha(t)+\alpha^\dagger(t)|+|\alpha(t)-\alpha^\dagger(t)|\right)}_{(C3)}\right)\mathcal{E}_N(t)\,.$$

Therefore, an outstanding task is to find a bound for $(C3)$. To this end, it is used that the formal solution for the scalar function $\alpha(t)$ is known and given by

$$\alpha(t)=\exp(-(i\delta-\kappa/2)t)\alpha(0)-\frac{ig}{\sqrt{2}}\int_0^t \mathrm{d}s\exp(-(i\delta-\kappa/2)(t-s))(m_x(s)-im_y(s))\,.$$

To find a upper bound for $|\alpha(t)|$, the conservation of the magnetization (i.e $m_x(t)^2+m_y(t)^2+m_z(t)^2=1/2$) is used, which results in the following expression for $|\alpha(t)|$

$$|\alpha(t)|\leq|\alpha(0)|+\frac{|g|}{\kappa}\,.$$

With $(C3)=|\alpha(t)+\alpha^\dagger(t)|+|\alpha(t)-\alpha^\dagger(t)|=2\mathrm{Re}(\alpha)+2\mathrm{Im}(\alpha)\leq 2|\alpha|=2\left(|\alpha(0)|+\frac{|g|}{\kappa}\right)$ follows that D_t^S is bounded by

$$\frac{S}{2}=6|\Omega|+3|\Delta|+12|g|+6|g|\left(|\alpha(0)|+\frac{|g|}{\kappa}\right)$$

and consequently

$$\left|\frac{\mathrm{d}}{\mathrm{d}t}\omega_t((m_a^N-m_a(t))^2)\right|\leq S\mathcal{E}_N(t)\,. \tag{46}$$

Bosonic operators In order to find a proper bound B for the bosonic mode the calculation of the derivative for the first contribution is the starting point

$$\frac{\mathrm{d}}{\mathrm{d}t}\left\langle\left(\alpha^N-\alpha(t)\right)^\dagger\left(\alpha^N-\alpha(t)\right)\right\rangle_t=D_t^B\,,$$

with

$$\begin{aligned}
D_t^B=&\left\langle\mathcal{L}^*\left[\left(\alpha^N-\alpha(t)\right)^\dagger\left(\alpha^N-\alpha(t)\right)\right]\right\rangle_t \\
&-\dot\alpha^\dagger(t)\left\langle\mathcal{L}^*\left[\alpha^N-\alpha(t)\right]\right\rangle_t-\dot\alpha(t)\left\langle\mathcal{L}^*\left[\left(\alpha^N-\alpha(t)\right)^\dagger\right]\right\rangle_t\,.
\end{aligned}$$

Due to the specific form of the adjoint Lindblad generator in Eq. (2), the first term of D_t^B can be written as follows

$$\mathcal{L}^*\left[\left(\alpha^N-\alpha(t)\right)^\dagger\left(\alpha^N-\alpha(t)\right)\right]=\mathcal{L}^*\left[(\alpha^N)^\dagger\right]\left(\alpha^N-\alpha(t)\right)+\left(\alpha^N-\alpha(t)\right)^\dagger\mathcal{L}^*\left[\alpha^N\right]\,.$$

Therefore the time-derivative is given by $D_t^B = \tilde{D}_t^B + (\tilde{D}_t^B)^*$, with

$$\tilde{D}_t^B = \left\langle \left(\mathcal{L}^* \left[(\alpha^N)^\dagger\right] - \dot{\alpha}^\dagger(t)\right)\left(\alpha^N - \alpha(t)\right)\right\rangle_t .$$

Eq. (45) and the corresponding mean-field equation results in

$$\mathcal{L}^* \left[(\alpha^N)^\dagger\right] - \dot{\alpha}^\dagger(t) = \left(i\delta - \frac{\kappa}{2}\right)\left((\alpha^N)^\dagger - \alpha^\dagger(t)\right) + \frac{ig}{\sqrt{2}}\left(-(m_x^N - m_x(t)) + i(m_y^N - m_y(t))\right) .$$

Inserting this expression back into the one for $\tilde{D}_t^B$ leads together with Lemma 1 from the supplemental material of [35] to

$$|\tilde{D}_t^B| \leq \underbrace{\left(\left(|\delta| + \frac{|\kappa|}{2}\right) + \sqrt{2}|g|\right)}_{B} \mathcal{E}_N(t) .$$

The second contribution of the bosonic mode to the cost function can be found by recalling the commutation relation $\left[\alpha, \alpha^\dagger\right] = 1/N$ for the mean-field operators. From

$$\begin{aligned} &\left\langle \left(\alpha^N - \alpha(t)\right)^\dagger \left(\alpha^N - \alpha(t)\right)\right\rangle_t = \left\langle \left(\alpha^N - \alpha(t)\right)\left(\alpha^N - \alpha(t)\right)^\dagger\right\rangle_t + \frac{1}{N} \\ \iff &\frac{\mathrm{d}}{\mathrm{d}t}\left\langle \left(\alpha^N - \alpha(t)\right)^\dagger \left(\alpha^N - \alpha(t)\right)\right\rangle_t = \frac{\mathrm{d}}{\mathrm{d}t}\left\langle \left(\alpha^N - \alpha(t)\right)\left(\alpha^N - \alpha(t)\right)^\dagger\right\rangle_t , \end{aligned}$$

follows that this term is bounded by the same constant B. All in all, the constant $C = 3S + 2B$, which does not depend on the number of two-level atoms N, bounds the time-derivative of the previously defined cost function

$$\frac{\mathrm{d}}{\mathrm{d}t}\mathcal{E}_N(t) = C\mathcal{E}_N(t) .$$

B. Stability analysis

The linearized expressions for the magnetization

$$m_y(t) \approx m_y^* + \delta m_y , \qquad m_z(t) \approx m_z^* + \delta m_z \qquad \text{and} \qquad m_p(t) \approx m_p^* + \delta m_p$$

are used to calculate the Jacobian matrix J, with $\frac{\mathrm{d}}{\mathrm{d}t}\boldsymbol{\delta m}(t) = J\boldsymbol{\delta m}(t)$. This is done by explicitly calculating the expressions $\dot{m}_c + \delta\dot{m}_c$, with $c = y, z, p$, and taking perturbations up to first-order into account. With the stationary solution the linearized Jacobian matrix takes the following form

$$J = \begin{pmatrix} 0 & 0 & -\sqrt{2}gm_z^* \\ 0 & 0 & \sqrt{2}gm_y^* \\ -g & 0 & -\frac{\kappa}{2} \end{pmatrix} .$$

The stationary solutions are now indeed stable if the real part of all eigenvalues of this matrix is smaller or equal to zero. The eigenvalues λ_i of the matrix J, with $\det(J - \lambda\mathbf{1})$, are given by

$$\lambda_1 = 0 \qquad \text{and} \qquad \lambda_{2,3} = -\frac{\kappa}{4}\left(1 \pm \sqrt{1 + \frac{4g^2\sqrt{2}m_z^*}{\left(\frac{\kappa}{2}\right)^2}}\right) .$$

Since the stationary solutions are only valid for $g > g_c$, this regime is the one of interest in the stability analysis. The insertion of the stationary solution for the magnetization in z-direction yields

$$\lambda_{2,3} = -\frac{1}{4}\left(1 \pm \sqrt{1 + 16 \cdot \pm\sqrt{\left(\frac{g}{\kappa}\right)^4 - \left(\frac{g_c}{\kappa}\right)^4}}\right) ,$$

where κ is set to one as before, which witnesses the instability of the positive stationary solution of m_z.

C. Time-evolution of the covariance matrix

In the following the explicit expressions for the different terms [cf. Eq. (18)] that contribute to the time-evolution of the matrix K^N are derived.

For the first part of Eq. (18) we start with the expression of the commutator [cf. Eq. (7)]

$$[H, F_a^N] \overset{a=x,y,z}{=} -2\Omega\varepsilon_{xac}\frac{V_c}{\sqrt{N}} + \Delta\varepsilon_{zac}\frac{V_c}{\sqrt{N}} - \sqrt{2}g\left(m_p^N\varepsilon_{xac} + m_q^N\varepsilon_{yac}\right)\frac{V_c}{\sqrt{N}}\,.$$

With this expression, fluctuation operators can be reconstructed by adding and subtracting different terms

$$\begin{aligned}
[H, F_a^N] &\overset{a=x,y,z}{=} -2\Omega\varepsilon_{xac}\left(\frac{V_c}{\sqrt{N}} - \frac{\langle V_c\rangle}{\sqrt{N}} + \frac{\langle V_c\rangle}{\sqrt{N}}\right) + \Delta\varepsilon_{zac}\left(\frac{V_c}{\sqrt{N}} - \frac{\langle V_c\rangle}{\sqrt{N}} + \frac{\langle V_c\rangle}{\sqrt{N}}\right)\\
&\quad - \sqrt{2}g\left(\frac{p}{\sqrt{N}} - \frac{\langle p\rangle}{\sqrt{N}} + \frac{\langle p\rangle}{\sqrt{N}}\right)\varepsilon_{xac}\frac{V_c}{\sqrt{N}} - \sqrt{2}g\left(\frac{q}{\sqrt{N}} - \frac{\langle q\rangle}{\sqrt{N}} + \frac{\langle q\rangle}{\sqrt{N}}\right)\varepsilon_{yac}\frac{V_c}{\sqrt{N}}\\
&= -2\Omega\varepsilon_{xac}\frac{F_c}{N} - 2\Omega\varepsilon_{xac}\frac{\langle V_c\rangle}{N} + \Delta\varepsilon_{zac}\frac{F_c}{N} + \Delta\varepsilon_{zac}\frac{\langle V_c\rangle}{N}\\
&\quad - \sqrt{2}gF_p^N\varepsilon_{xac}m_c^N - \sqrt{2}g\frac{\langle p\rangle}{\sqrt{N}}\varepsilon_{xab}\left(\frac{V_c}{\sqrt{N}} - \frac{\langle V_c\rangle}{\sqrt{N}} + \frac{\langle V_c\rangle}{\sqrt{N}}\right)\\
&\quad - \sqrt{2}gF_q^N\varepsilon_{yac}m_c^N - \sqrt{2}g\frac{\langle q\rangle}{\sqrt{N}}\varepsilon_{yac}\left(\frac{V_c}{\sqrt{N}} - \frac{\langle V_c\rangle}{\sqrt{N}} + \frac{\langle V_c\rangle}{\sqrt{N}}\right)\\
&= -2\Omega\varepsilon_{xac}\frac{F_c}{N} - 2\Omega\varepsilon_{xac}\frac{\langle V_c\rangle}{N} + \Delta\varepsilon_{zac}\frac{F_c}{N} + \Delta\varepsilon_{zac}\frac{\langle V_c\rangle}{N}\\
&\quad - \sqrt{2}gF_p^N\varepsilon_{xac}m_c^N - \sqrt{2}g\frac{\langle p\rangle}{\sqrt{N}}\varepsilon_{xac}F_c^N - \sqrt{2}g\frac{\langle p\rangle}{\sqrt{N}}\varepsilon_{xac}\frac{\langle V_c\rangle}{\sqrt{N}}\\
&\quad - \sqrt{2}gF_q^N\varepsilon_{yac}m_c^N - \sqrt{2}g\frac{\langle q\rangle}{\sqrt{N}}\varepsilon_{yac}F_c^N - \sqrt{2}g\frac{\langle q\rangle}{\sqrt{N}}\varepsilon_{yac}\frac{\langle V_c\rangle}{\sqrt{N}}\,.
\end{aligned}$$

The terms containing only scalars will not contribute to $\langle i[H, F_a^N]F_b^N\rangle$ since the expectation values of fluctuation operators are zero (i.e. $\langle F_b^N\rangle = 0$). This leads for the fluctuations operators of the atoms to the following expression

$$\begin{aligned}
\langle i[H, F_a^N]F_b^N\rangle &\overset{a=x,y,z}{=} -2\Omega\varepsilon_{xac}\langle F_c^N F_b^N\rangle + \Delta\varepsilon_{zac}\langle F_c^N F_b^N\rangle - \sqrt{2}g\varepsilon_{xac}\langle F_p^N m_c^N F_b^N\rangle\\
&\quad - \sqrt{2}g\frac{\langle p\rangle}{\sqrt{N}}\varepsilon_{xac}\langle F_c^N F_b^N\rangle - \sqrt{2}g\varepsilon_{yac}\langle F_q^N m_c^N F_b^N\rangle - \sqrt{2}g\frac{\langle q\rangle}{\sqrt{N}}\varepsilon_{yac}\langle F_c^N F_b^N\rangle\,.
\end{aligned}$$

It will be used that in the thermodynamic limit $\lim_{N\to\infty}\langle F_a^N m_c^N F_b^N\rangle = m_c(t)\langle F_a F_b\rangle$, with the mean-field observable $m_c(t)$. For the fluctuation operators of the bosonic mode of the cavity the following expression can be obtained

$$\begin{aligned}
\langle i[H, F_a^N]F_b^N\rangle &\overset{a=q,p}{=} \langle ig\left[m_p^N V_x + m_q^N V_y, F_a^N\right]F_b^N\rangle + \langle -i\delta[a^\dagger a, F_a^N]F_b^N\rangle\\
&= \begin{cases} -g\langle F_y^N F_b^N\rangle + \delta\langle F_q^N F_b^N\rangle & F_a^N = F_p^N\,,\\ g\langle F_x^N F_b^N\rangle - \delta\langle F_p^N F_b^N\rangle & F_a^N = F_q^N\,,\end{cases}
\end{aligned}$$

by directly evaluating the appearing commutator. All in all, the time-evolution of the matrix K due to the Hamiltonian is given by

$$\lim_{N\to\infty}\langle i\left[H, F_a^N\right]F_b^N\rangle = (PK)_{ab}\,,$$

with

$$P(t) = \begin{pmatrix} 0 & \Delta & \sqrt{2}gm_q(t) & \sqrt{2}gm_z(t) & 0\\ -\Delta & 0 & -2\Omega - \sqrt{2}gm_p(t) & 0 & -\sqrt{2}gm_z(t)\\ -\sqrt{2}gm_q(t) & 2\Omega + \sqrt{2}gm_p(t) & 0 & -\sqrt{2}gm_x(t) & \sqrt{2}gm_y(t)\\ g & 0 & 0 & 0 & -\delta\\ 0 & -g & 0 & \delta & 0\end{pmatrix}\,.$$

For the second term in Eq. (18) one analogously derive the following expression

$$\lim_{N\to\infty} \left\langle iF_a^N \left[H, F_b^N\right]\right\rangle = (KP^T)_{ab}\,.$$

For the dissipative part it is used that the product of two fluctuation operators can be rewritten in the following way

$$\mathcal{D}\left[F_a^N F_b^N\right] = F_a^N \mathcal{D}\left[F_b^N\right] + \mathcal{D}\left[F_a^N\right] F_b^N + \kappa\left[a^\dagger, F_a^N\right]\left[F_b^N, a\right]\,,$$

such that

$$\lim_{N\to\infty} \left\langle \mathcal{D}\left[F_a^N F_b^N\right]\right\rangle = (KEs)_{ab} + (sEK)_{ab} - (sE's)_{ab}\,,$$

with

$$E = \frac{\kappa}{2}\begin{pmatrix} 0 & 0 & 0 & 0 & 0\\ 0 & 0 & 0 & 0 & 0\\ 0 & 0 & 0 & 0 & 0\\ 0 & 0 & 0 & 0 & 1\\ 0 & 0 & 0 & -1 & 0 \end{pmatrix} \qquad \text{and} \qquad E' = \frac{\kappa}{2}\begin{pmatrix} 0 & 0 & 0 & 0 & 0\\ 0 & 0 & 0 & 0 & 0\\ 0 & 0 & 0 & 0 & 0\\ 0 & 0 & 0 & 1 & i\\ 0 & 0 & 0 & -i & 1 \end{pmatrix}.$$

By rewriting the bosonic creation and annihilation operators in terms of the quadrature operators, the following Kossakowski matrix for the dissipator

$$C = \frac{\kappa}{2}\begin{pmatrix} 0 & 0 & 0 & 0 & 0\\ 0 & 0 & 0 & 0 & 0\\ 0 & 0 & 0 & 0 & 0\\ 0 & 0 & 0 & 1 & i\\ 0 & 0 & 0 & -i & 1 \end{pmatrix},$$

can be regained. Therefore, $E' = C = A + iB$ and $E = B$. As a result the time-evolution of the covariance matrix is

$$\begin{aligned}\dot{\Sigma} &= \frac{\dot{K} + (\dot{K})^T}{2}\\ &= \frac{\left(PK + KP^T + KBs + sBK - sCs\right) + \left(K^T P^T + PK^T + s^T B^T K^T + K^T B^T s^T - s^T C^T s^T\right)}{2}\\ &= (P + sB)\Sigma + \Sigma(P^T + Bs) - \frac{sCs + s^T C^T s^T}{2}\\ &= W\Sigma + \Sigma W^T + sAs^T\,.\end{aligned}$$